THE APPLICATION OF SYNTHESIZED TRANSITION METAL COMPOUNDS AS PAINT ADDITIVES FOR THE PREPARATION OF A SELF-DECONTAMINATING COATING

By

Spencer Lawrence Giles

RECOMMENDED: _____

_____

_____
Advisory Committee Chair

_____
Chair, Department of Chemistry and Biochemistry

APPROVED: _____
Dean, College of Natural Science and Mathematics

_____
Dean of the Graduate School

_____
Date

THE APPLICATION OF SYNTHESIZED TRANSITION METAL COMPOUNDS AS PAINT ADDITIVES FOR THE PREPARATION OF A SELF-DECONTAMINATING COATING

A

THESIS

Presented to the Faculty

of the University of Alaska Fairbanks

in Partial Fulfillment of the Requirements

for the Degree of

MASTER OF SCIENCE

By

Spencer Lawrence Giles, B.S.

Fairbanks, Alaska

August 2011

Abstract

The synthesis of transition metal compounds has been performed to create reactive additives that can be incorporated into commercial grade paints for the purpose of developing a continuous self-decontaminating coating. The coatings were designed to allow for the decontamination of persistent chemical warfare agents: sulfur mustard and organophosphate nerve agents. Since the persistence of these chemicals on surfaces due to their low volatility and long hydrolysis half lives could possibly lead to involuntary exposures, a continuous self-decontaminating coating would provide an alternative approach to eliminate residual chemical warfare agents without further treatment to the painted surface. The synthesized additives include metal oxide nanoparticles, polyoxometallates, and metal functionalized cyclodextrins. Coatings were formulated with 1% w/w synthesized additives, and tested for their ability to decontaminate chemical warfare agent simulants of sulfur mustard and organophosphate nerve agents. The Dawson structure polyoxometallate α_2-$K_8P_2W_{17}O_{61}(Ni^{2+} \cdot OH_2) \cdot 17H_2O$ coatings exhibited percent reductions of three of the four simulants above 30% with a high of 53% reduction of Malathion in 24 hours. The nickel functionalized gamma cyclodextrin coatings exhibited percent reductions for all simulants above 28% with a high of 61% reduction of Malathion in 24 hours. Overall, coatings enhanced with additives were tested and produced painted surfaces capable of decontaminating chemical warfare agent simulants.

Table of Contents

Page

List of Figures

Page

List of Tables

Page

List of Abbreviations

AChE – acetylcholinesterase

CD – Cyclodextrin

CEES – 2-Chloroethyl ethyl sulfide

CEPS – 2-Chloroethyl phenyl sulfide

CWAs – Chemical Warfare Agent

DS2 – Decontamination Solution 2

GA – Tabun

GB – Sarin

GD – Soman

GC/MS – Gas Chromatography/Mass Spectrometry

HD – Sulfur Mustard Distilled, Bis(2-chloroethyl)sulfide

MONPs – Metal Oxide Nanoparticles

OP – Organophosphate

POMs – Polyoxometallate

VX – O-ethyl S-[2-diisopropylaminoethyl] methylphosphonothioate

Acknowledgements

At the University of Alaska Fairbanks I would like to thank Dr. Brian Rasley for all the help over the length of the project as well as being the chair of my graduate advisory committee. Dr. Thomas Green for participating as a committee member as well as providing help with the cyclodextrin research conducted. I would also like to thank Dr. Daniel Kirschner and Michael Jaramillo for their help and advice with respect to working with cyclodextrins in the laboratory.

At the Naval Research Laboratory I would like to thank Dr. James Wynne for participating as a committee member as well as providing help with coatings applications. Jeffrey Lundin for coatings formulation as well as application and chemical warfare agent simulant challenge testing. I would also like to thank Kelly Watson for the GC/MS analysis for the simulant challenge testing.

Funding for the research conducted was provided by the Naval Research Laboratory and Defense Threat Reduction Agency – Joint Science and Technology Office under the award number N00173-08-1-G008.

Dedication

To my loving wife, Carlise and our beautiful daughter, Sydney

Chapter 1 : Background

1.1 Introduction

The public deployment of Sarin (GB), a chemical warfare agent (CWA), in 1994 and 1995 by a terrorist group in Japan illustrates the threat currently posed by chemical weapons.[1] These types of CWAs not only pose a direct threat to those exposed at the time of deployment, but also those who may come into contact with residual CWAs left on unwashed surfaces. The cleaning challenge related to these types of chemicals has been a work in progress throughout many years and is still a major issue to date. The major challenge posed by certain CWAs is their persistence in the environment once released. Due to the large stockpiles of CWAs and the elevated threat of terrorism, there is a need for the development of safe and effective decontamination methods that can be employed if some disaster occurs.[2] Currently the decontamination methods utilized are quite corrosive and harmful to any machinery being cleaned as well as the personnel performing the cleanup.[3,4] In an effort to reduce the use of aggressive processes for cleanup of CWA releases, the development of a chemically active coating has been undertaken to produce a continuous self-decontaminating surface. The active coating approach would promote contact cleaning of the surface without the necessity of decontamination solutions. The approach of reactive coatings has also been employed for other surface applications in the past with some success. Anti-fouling coatings have been used to increase fuel efficiency for vessels at sea by preventing build up of bio-fouling on ship hulls.[5] Anti-microbial coatings employed to kill bacteria are

also in development and could be employed in hospitals and other high traffic areas to prevent bacteria from spreading.[6]

1.2 Chemical Warfare Agents

Chemical warfare agents can be defined as weapons of chemical origin designed to be used to exploit the inherent hazardous properties of the chemicals.[7] The modern use of chemical warfare agents began in World War I with the use of chlorine gas by the German Army at Ypres on April 22, 1915.[1,7,8] Since the first deployment of chlorine gas, chemical weaponry has evolved from asphyxiation chemicals to more advanced and far more dangerous chemicals such as O-ethyl S-[2-diisopropylaminoethyl] methylphosphonothioate (VX) a nerve agent which affects the central nervous system.

The CWAs of interest for the current study are considered to be persistent in the environment due to their low vapor pressure and their long hydrolysis half lives. This persistence is the driving force behind the research in this study because of the added challenges these CWAs present in cleanup procedures. Table 1.1 illustrates some of the physical properties for the CWAs of interest as well as the inherent mode of action for which each chemical is utilized for as a weapon.[3]

Table 1.1: Chemical Warfare Agent Properties (T = 20 – 25 °C pH = 6.6 – 8.6)

CWA	Mode of Action	Solubility in Water (g/L)	Vapor Pressure (mm Hg)	Hydrolysis Half-Life
HD; Sulfur Mustard	Vesicant	0.92	0.11	8.5 min
GA; Tabun	Nerve Agent	98	0.07	8.5 hrs
GB; Sarin	Nerve Agent	Miscible	2.10	39 – 125 hrs
GD; Soman	Nerve Agent	21	0.40	5.25 hrs
VX	Nerve Agent	30	0.0007	41 days

The short hydrolysis half-life of 8.5 minutes for sulfur mustard might lead one to believe that sulfur mustard is not very persistent in the environment. However the persistence of sulfur mustard arises from its low solubility in water, 0.92 g/L, which means that less of the sulfur mustard is able to react with water at any given time. The ability of these CWAs to reside on surfaces for long periods of time could lead to secondary routes of exposure long after the initial deployment. The possibility of employing a functional coating for decontamination purposes like those coatings used in anti-fouling and anti-bacterial applications could resolve the issue of long residence times on surfaces.

1.2.1 Vesicants

A vesicant is defined as a chemical agent that causes burns and destruction of tissue.[9] Vesicant CWAs are known as blistering agents and cause severe damage to the exposed areas of the human body. The main vesicant of concern for the present study is sulfur mustard (HD; bis(2-chloroethyl)sulfide) shown in Figure 1.1.

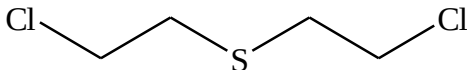

Figure 1.1: Sulfur Mustard (HD; bis(2-chloroethyl)sulfide

Sulfur mustard was first discovered in 1822 by Despretz without the knowledge of the inherent toxicity of the compound. Later in 1860 crude sulfur mustard was synthesized simultaneously by Guthrie in the United Kingdom and by Niemann in Germany. The first purified sample of sulfur mustard was reported much later in 1886 by Meyer.[7] Sulfur mustard was first utilized as a CWA in World War I and has been subsequently utilized in the recent Iran-Iraq war. Therefore, due to the elevated threat of terrorism, sulfur mustard decontamination is still a priority.[7,10,11]

Sulfur mustard was specifically developed as a CWA and has been utilized as such due to the strong alkylation reaction pathways exhibited. The inherent toxicity of sulfur mustard comes from the formation of the sulfonium cation, shown in Figure 1.2, which acts as an alkylation agent.[12,13]

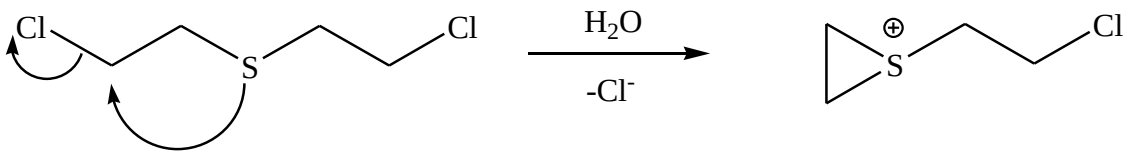

Figure 1.2: Formation of the sulfonium ion (right) from sulfur mustard (left)

The sulfonium ion shown in Figure 1.2 reacts as a strong electrophile thereby forming alkylation adducts with many nucleophilic groups. This reactivity leads to alkylation of a

majority of macromolecules leading to cross linked DNA or proteins which alters the functionality of the macromolecules.[10,11,13,14] Although the reactivity of sulfur mustard is fairly high, the lethality is quite low at about 2% but this is dependent upon the mode and location of exposure to sulfur mustard.[7]

1.2.2 Nerve Agents

The second major class of CWAs is nerve agents which consist of organophosphate (OP) chemical compounds that affect the central and peripheral nervous systems. Nerve agents act as irreversible acetylcholinesterase (AChE) inhibitors by phosphorylation of the hydroxyl group of the serine residue in the active site of the enzyme as illustrated in Figure 1.3.[7,15-17]

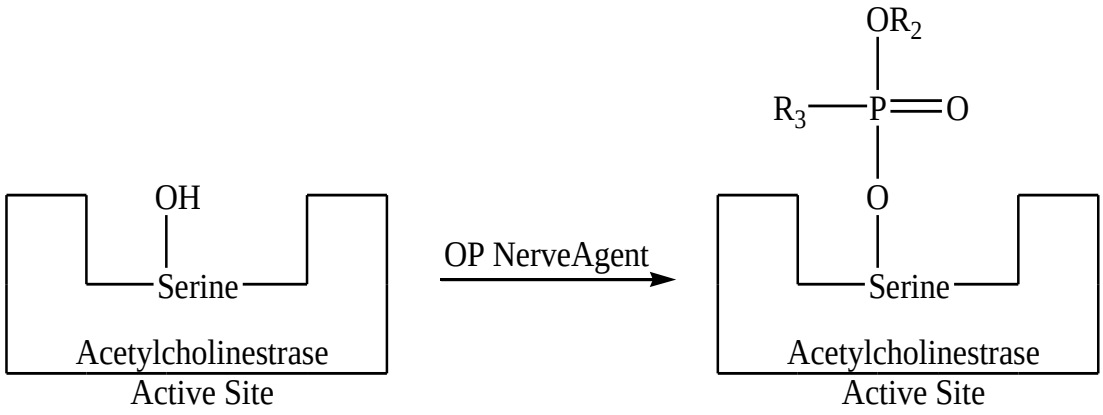

Figure 1.3: Phosphorylation of the AChE active site serine by OP nerve agent

The inhibition of the AChE leads to the accumulation of the neurotransmitter acetylcholine which causes overstimulation of the nervous system leading to cholinergic syndrome in the victim.[15] Once the nerve agent has bound to the serine residue in the

active site, the reactivation of the enzyme is dependent upon the substituent groups R_2 and R_3 as seen in Figure 1.3. The larger the substituent groups are the more difficult and longer the reactivation process will take because of limited access to the O-P bond. The speed of irreversible binding exhibited by OP nerve agents is referred to as aging. Aging is the amount of time required to dealkylate the bound agent creating a stronger OP-enzyme complex.[15] The faster the OP-enzyme complex ages the quicker treatment needs to be applied to act against the OP poisoning. Organophosphate poisoning is treated with a mixture of atropine, an anticholinergic, and oximes, an AChE reactivation chemical, which blocks acetylcholine from further binding to the receptors and facilitates the release of the bound OP.[7,15]

The nerve agents of concern in the current study are listed in Table 1.1 and can be split into two groups, G-agents and V-agents. The development of the G-agents began in the 1930s with studies being conducted into organophosphate insecticides and continued through the 1940s in Germany during World War II after the inherent toxicities of the compounds was discovered.[7] The three G-series agents of interest listed in Table 1.1 are Tabun (GA), Sarin (GB), and Soman (GD) whose structures are shown in Figure 1.4.

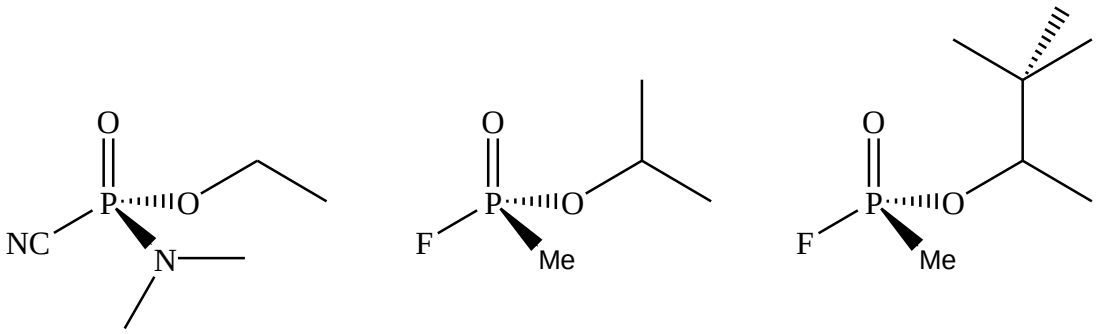

Tabun (GA) Sarin (GB) Soman (GD)

Figure 1.4: Structural representations of the G-series nerve agents

Figure 1.4 illustrates the structural representations of the G-agents with specific stereochemistry around the phosphorus atom; however these compounds have enantiomers and exist as racemic mixtures. The G-agents are not quite as persistent as the V-agents based upon the vapor pressures and hydrolysis half-lives listed in Table 1.1. Sarin (GB) has the highest vapor pressure at 2.10 mmHg and is the most volatile of the G-agents while Soman (GD) has the fastest hydrolysis half-life at 5.25 hours meaning the breakdown in water is fairly quick. Compared to VX the G-agents are not very persistent when compared to the low vapor pressure of 0.0007mmHg and the long hydrolysis half-life of 41 days for VX.

The pinnacle of chemical warfare is the nerve agent VX. VX has the longest hydrolysis half-life as well as the lowest vapor pressure of all of the nerve agents listed in Table 1.1. The structure of VX and the Russian VX analogue, shown in Figure 1.5, are similar to those of the G-series agents with one minor change and that is the replacement of the simplistic groups (fluorine, cyanide) with a large thioether group.

Figure 1.5 also illustrates specific stereochemistry for both VX and Russian VX, but both are racemic with their respective enantiomers. The current study focuses on VX, however any research conducted on VX is believed to be applicable to the Russian VX analog as well.

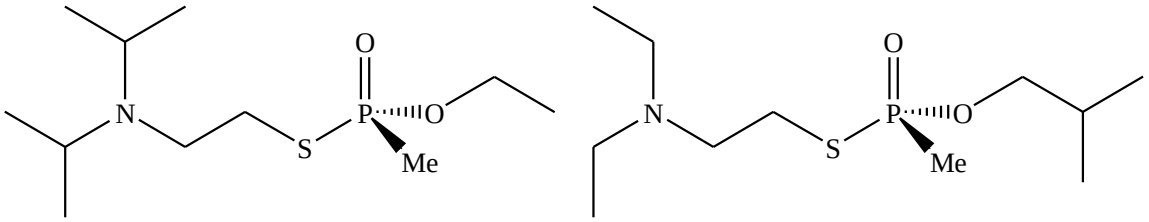

VX Russian VX

Figure 1.5: Structural representations of VX and Russian VX nerve agents

The development of VX began after World War II in the early 1950s with full production beginning in the 1961 and running to 1968.[18] The estimated lethal dose of VX is thought to be 0.3 mg/person when inhaled and 5 mg/person via dermal exposure.[7]

1.3 Chemical Warfare Agent Simulants

The use of CWAs in the laboratory is very restricted and only few places are allowed to handle and use CWAs due to their lethality if even slightly mishandled.[17,19] Due to the limited access to CWAs for testing applicable model compounds known as simulants are tested in place of CWAs. The CWA simulants allow for approximate reactivity schemes as well as maintaining a safe laboratory environment. Several criteria need to be met when considering a compound for use as a CWA simulant. The first criterion is that the simulant must have similar chemical structure (with

stereochemistry) and exhibit similar reactivity toward oxidation, reduction and acid base interactions. Second, the simulant needs to maintain similar physical and chemical properties such as vapor pressure, surface tension and polarity for accurate surface interaction modeling. The third and final criterion the simulants must exhibit is reduced toxicity to maintain a safe laboratory environment. A single CWA simulant may not model the CWA perfectly; however multiple CWAs can be utilized to investigate the properties of CWAs in order to better understand the complete reactivity of the CWA.[4,20]

Simulants for sulfur mustard utilized in the current study are 2-chloroethyl ethyl sulfide (CEES) and 2-chloroethyl phenyl sulfide (CEPS) illustrated in Figure 1.6.

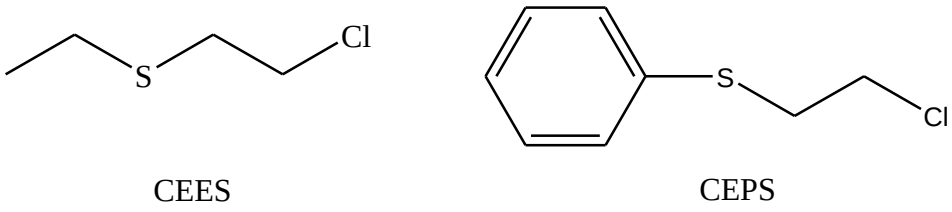

CEES CEPS

Figure 1.6: HD simulants 2-chloroethyl ethyl sulfide (left) and 2-chloroethyl phenyl sulfide (right)

Both of the simulants shown are utilized for their ability to form the sulfonium ion by loss of the chlorine atom similar to that of HD as shown in Figure 1.2. The physical and chemical properties shown in Table 1.2 outline the similarities these compounds have in comparison to HD.

Table 1.2: Physical chemical properties of HD compared to CEES and CEPS

	HD	CEES	CEPS
Molecular Weight (g/mol)	159	125	173
Liquid Density (g/cm^3 @ 20°C)	1.27	1.04	1.16
Boiling Point (°C @ 750 mmHg)	216	156	246
Vapor Pressure (mmHg @ 25 °C)	0.11	3.79	0.0443
Surface Tension (dyne/cm)	34.7	29.8	40.7

Structurally, CEES is most similar to HD and offers similar chemical reactivity as well as similar surface tension. These similarities indicate that CEES should have similar contact with the surface on which the residual chemical resides as well as similar degradation pathways.[21,22] However CEPS better related to HD with regard to vapor pressure and displays similar volatility and retention times on untreated surfaces after deposition.[23] Both of these simulants have been utilized in the past as model compounds for degradation experiments with some success.[23-26]

Simulants for VX are very numerous due to the abundance of organophosphate pesticides and other organophosphate compounds.[15,23] Two organophosphate insecticides were chosen as simulants based upon their similar structural and physical properties to VX. The structures of VX, Malathion, and Demeton-S are shown in Figure 1.7 without stereochemistry and illustrate the similar structural characteristics.

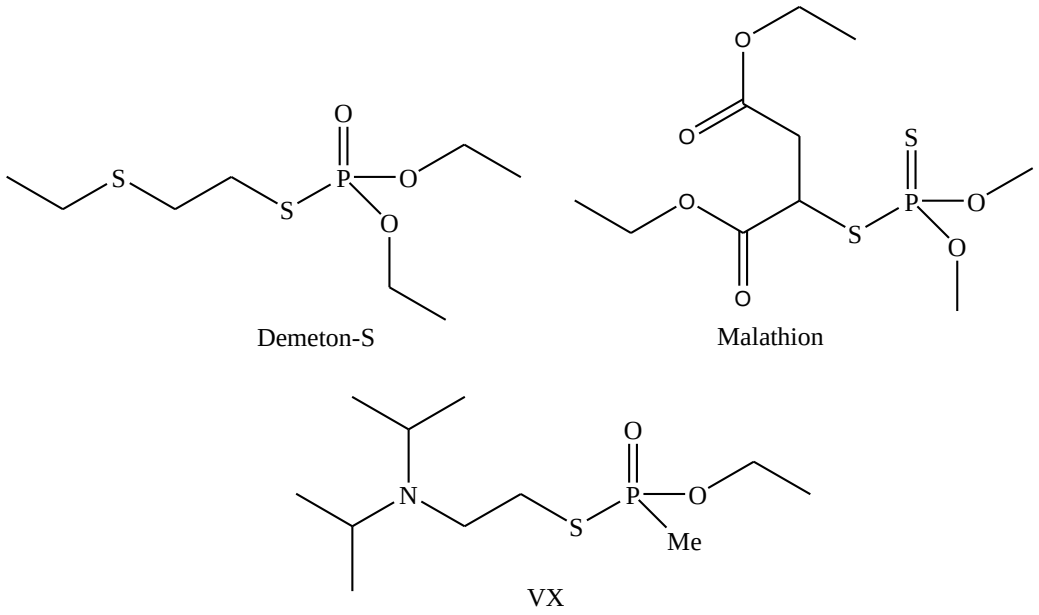

Figure 1.7: Structural representations of Demeton-S and Malathion compared with VX

Each of the simulants contains the phosphonothioate P-S bond which is a primary target for oxidative decontamination of VX.[2,4,27] The presence of the methoxy and ethoxy groups also enhances the effectiveness of the model due to the presence of an ethoxy group in the VX molecular structure. Table 1.3 shows the comparison of some of the important physical chemical properties of VX, Malathion, and Demeton-S.

Table 1.3: Physical chemical properties of VX, Malathion and Demeton-S

	VX	Malathion	Demeton-S
Molecular Weight (g/mol)	267.4	330.4	258.3
Liquid Density (g/cm^3 @ 20°C)	1.018	1.272	1.146
Boiling Point (°C @ 750 mmHg)	319	385.1	321
Vapor Pressure (mmHg @ 25 °C)	7.0×10^{-4}	3.9×10^{-6}	5.95×10^{-4}
Surface Tension (dyne/cm)	33.6	47.1	38.9

Both VX simulants exhibit similar physical and chemical properties of interest including very low vapor pressures. The low vapor pressures indicate that the chemical will not volatilize at typical pressures and temperatures, therefore the chemicals will remain present on the surface long after initial deposition. The similar surface tensions shown in Table 1.3 indicate that the compounds will interact with the surfaces on which they reside in similar ways.[21,22] Both Malathion and Demeton-S are commercially available insecticides with greatly reduced toxicity (compared to V-agents) for laboratory testing of reactive coatings.

1.4 Decontamination of CWAs

The driving force behind the present research in CWA decontamination is the speed, ease and effectiveness of field decontamination of equipment after CWA exposure. Historically decontamination of CWAs dates back to World War I with the first use of sulfur mustard (HD). Prior to the first use of HD, all other chemical warfare

agents were gaseous weapons such as chlorine and phosgene which dissipated with time.[4,7,8] Bleaching powders and solutions were utilized to decontaminate CWAs up until the end of World War II with the discovery of the German G-agents. The main problem with bleaching powders and solutions is their corrosive effect on certain materials.[4] Along with the corrosive effects on materials bleaching agents do not store very well and are not very effective at cold temperatures. The answer to cold temperatures and length of storage was solved by the creation of Decontamination Solution 2 (DS2) which could be stored for long periods of time and could be utilized in the cold of winter. DS2 however was still corrosive towards certain materials as well as personnel performing the cleanup.[3,4] Currently, decontamination solutions are moving toward "green" chemistry through the use of peroxides, the use of radical based systems and enzymatic pathways for decontamination.[3,12,28-30]

1.5 Functional Coating Applications

There has been considerable evolution of the modern decontamination solution however a smaller effort has been dedicated toward the modification of polymers and coatings systems for enhanced reactivity toward CWA on the surface to which they are applied. In a recent study on Nomex®, a polymer textile, was modified with N-chloramide and loaded with chlorine using sodium hypochlorite (NaOCl) showed promising results of decontamination against CEES and Demeton-S.[19] In another report, nucleophilic hydrolysis of organophosphate CWAs was reported by using polyacrylamidoxime (PANOx) and poly(N-hydroxyacrylamide) (PHA), both reactive

polymers.[31] The use of additives in coatings systems to create reactive surfaces has been demonstrated in the literature with the formulation of antifouling paints and anti-microbial resin systems. The key to the formation of a continuous decontamination surface is the selection of the proper additives for intended purpose and whether or not the additives adversely affect the paint system employed. The coating system utilized in the current study is a two component polyurethane paint MIL-PRF-85285 and the reactive additives are metal oxide nanoparticles, polyoxometallates, and metal functionalized cyclodextrins. These additives will be incorporated into MIL-PRF-85285 in a 1% w/w additive to paint ratio and tested for their decontamination capabilities toward the CWA simulants listed in Section 1.3.

1.6 MIL-PRF-85285 Coating

The coating system MIL-PRF-85285 is a two component high solids solvent borne polyester based urethane. The system consists of a hydroxyl terminated aliphatic polyester cross-linked with an aliphatic hexamethylene diisocyanate (HDI) based polyisocyanate. The MIL-PRF-85285 coating was chosen because the durability as well as the applicability to multiple substrates. MIL-PRF-85285 is able to withstand physical stress (scratching, cracking, puncture), withstands most chemical solvents, is affordable, has a wide operational temperature range, and is capable of adherence to steel and aluminum. Most importantly however is the ability of MIL-PRF-85285 to be compatible with a variety of chemical additives which is vital to the current study. MIL-PRF-85285 meets all the standard requirements set forth by the United States military for

application as a topcoat for fixed wing aircraft in both the Navy and Air Force. The key factor to modification of existing coatings systems, especially for the current research, is to maintain the characteristic properties the coating system already exhibits while enhancing the decontamination properties toward CWAs.

1.7 Metal Oxide Nanoparticles

Metal oxide nanoparticles (MONPs) have shown great success in many areas of chemistry and physics.[32] In the realm of the current study, metal oxide nanoparticles could provide an affordable option as paint additives if they are successful. Due to the abundant pathways of MONP synthesis there are countless numbers of MONP options which could be utilized toward the creation of a continuous self-decontamination coating.[32,33] Metal oxides MgO, CaO and nanotubular titania have shown potential as absorbents for the decontamination of CWAs of interest due to high surface areas with quick reaction times toward the contaminants.[34-36] Surface functionalized magnetite (Fe_3O_4) has also been utilized as an OP CWA decontaminant which can be recovered after use in solution due to the inherent magnetic properties.[37,38] Overall MONP show promise toward the development of a continuous self-decontamination surface by exhibited reactivity with CWAs and CWA simulants shown in the literature. MONP are also very simple to synthesize and are commercially available making MONP a cheap and simple option for additives.[39,40]

1.8 Polyoxometallates

Polyoxometallates (POMs) are metal-oxygen cage structure molecules that have been used as catalysts and in other applications due to the ability to substitute hetero-metal atoms into the cage structure.[41-46] These substitutions enhance the reactivity while maintaining a solid base structure. There are multiple cage structure families of POMs which include the Keggin ($XM_{12}O_{40}^{n-}$) and Dawson ($X_2M_{18}O_{62}^{n-}$) structures shown in Figure 1.8. Keggin and Dawson type POMs were utilized in the current study.

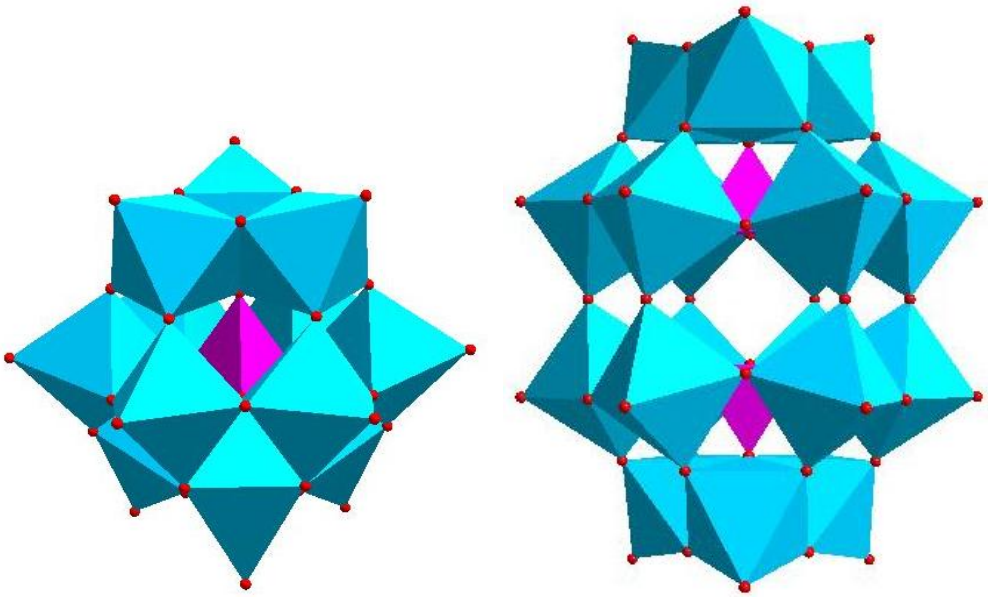

Figure 1.8: Structural representations of the Keggin (left) and Dawson (right) POMs

In Figure 1.8 and from the formulas, X represents the central atom which is phosphorus, M represents the octahedrons which are tungsten and the small spheres represent the oxygen atoms. Multiple polyoxometallates have also been shown in the literature to be

affective against decontamination and detection of CWAs making them possible candidates as reactive additives.[24-26,47]

1.9 Metal Functionalized Cyclodextrins

Cyclodextrins (CDs) have also been considered for the current research as possible additives based upon their abilities to form inclusion complexes with organic molecules. Organic compounds are capable of fitting into the hydrophobic cavity formed by the glucose units.[48-50] There are three commercially available CDs alpha (α), beta (β) and gamma (γ) (shown in Figure 1.9) having six, seven and eight glucose units, respectively.

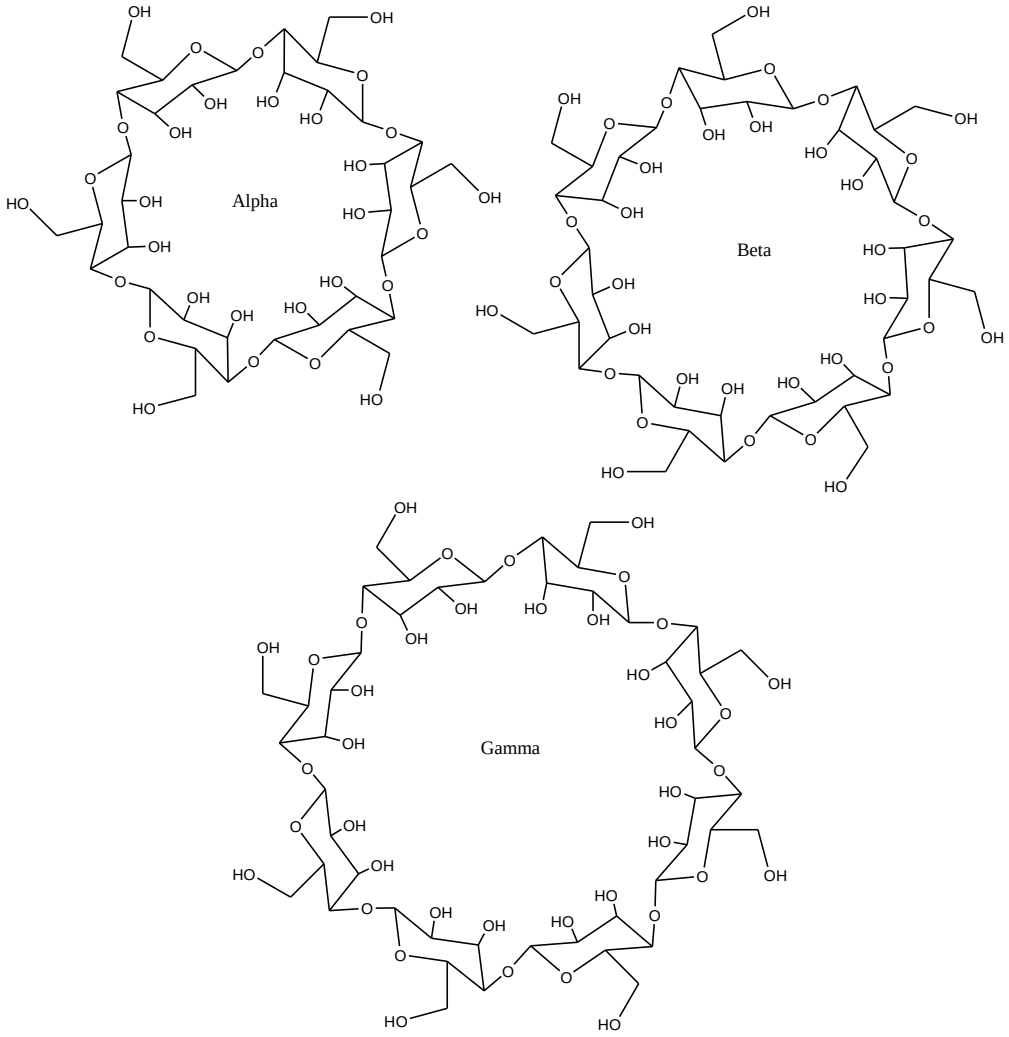

Figure 1.9: Structural representations of alpha (top left), beta (top right), and gamma (bottom) cyclodextrins

The macrocycle structures of the cyclodextrins shown in Figure 1.9 have three dimensional structures which resemble truncated cones as shown in Figure 1.10.[51] The structures have two interfaces (primary and secondary) formed by the alignment of the cyclodextrin hydroxyl groups. The primary hydroxyl groups, forming the outside rings of each cyclodextrin shown in Figure 1.9, align to form the lower part of the truncated

cone as shown in Figure 1.10. The secondary hydroxyl groups, forming the inside ring of each cyclodextrin shown in Figure 1.9, align to form the upper part of the truncated cone shown in Figure 1.10.

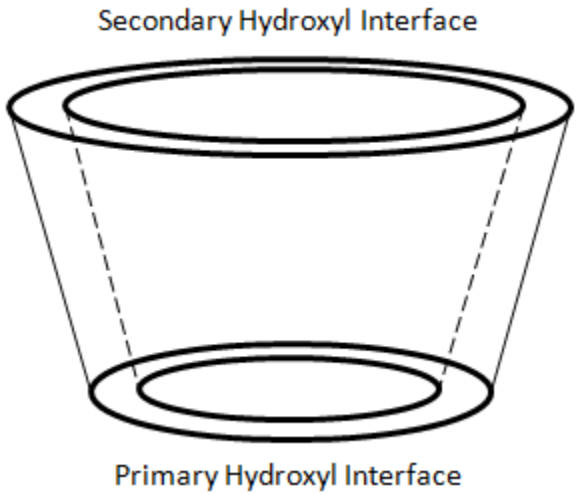

Figure 1.10: Visual representation of CD truncated cone formed by the glucose unit

The cone structure provides the hydrophobic cavity for the formation of organic inclusion complexes, and the different available CDs allows for variations in the overall cavity size. The cyclodextrin hydroxyl groups (primary and secondary) are also capable of being functionalized allowing for a multitude of possible decontamination additives.[52-57] The unique characteristics of cyclodextrins have been utilized in decontamination and surface cleanup of CWAs making them great candidates as additives for decontamination.[56,58]

Chapter 2 : Synthesis and Coatings Characterization

2.1 Synthetic Overview

One of the major guidelines involved in the current research has been the affordability of the additives. A second priority is the ease to which the additives are synthesized. Synthetically, the most affordable and simplest additives require the least amount of specialized materials and equipment. Simple synthetic routes with standard reagents would be ideal if the products were successful in the CWA challenge experiments. In undertaking the research, affordability was first and foremost in the selection of the additive types produced. The synthetic techniques utilized in the current research involved standard bench top practices, standard Schlenk techniques and high pressure vessels for hydrothermal reactions.

The current chapter outlines the synthetic approaches and coatings analysis techniques utilized in the current study. Full synthetic and coatings analysis details are provided in Chapter 3.

Standard Schlenk techniques require the utilization of a Schlenk line as depicted in Figure 2.1.

Figure 2.1: Schlenk line utilized for inert atmosphere reactions

A Schlenk line is a two manifold system utilized for evacuation and purging of a reaction vessel to produce an inert atmosphere. One manifold leads to a vacuum pump equipped with a liquid nitrogen trap for evacuation of the reaction vessel. The second manifold leads to a purge tank of inert gas used to maintain an inert atmosphere in the reaction vessel. The Schlenk line is an alternative for working in an inert atmosphere without an expensive inert atmosphere glove box.

The high pressure vessel for hydrothermal reactions utilized in the current work was a Parr Instrument Company bomb calorimeter shown in Figure 2.2.

Figure 2.2: Parr Instrument Company bomb calorimeter utilized for high pressure reactions

Hydrothermal reactions requiring high pressures were sealed inside the calorimeter fitted with Teflon® liner.

2.2 Metal Oxide Nanoparticles

Metal oxide nanoparticles (MONPs) are structurally and synthetically the simplest additives tested. There are three general synthetic pathways toward the synthesis of MONPs: solids, aqueous sol-gel, and non-aqueous.[32] The use of solids to react and form metal oxides required high temperatures and pressures without much control over the final product morphologies. Aqueous sol-gel methods are unreliable based upon the complexity of the aqueous chemical system and the constant changes in products based upon miniscule changes in the reaction parameters. Non-aqueous reaction chemistries allow for control over the morphologies as well as the size of the

particles at low temperatures with some instances of great success shown in the literature.[32,39,40]

In the current study, non-aqueous methods were used based upon the ease and reliability of the reaction parameters set out in the literature. Three metal oxides were synthesized in the current work: iron oxide (Fe_3O_4), zinc oxide (ZnO), and titanium dioxide (TiO_2). Each of the reaction systems involved the utilization of benzyl alcohol and the corresponding metal halide or metal acetate. These reactions were performed using standard Schlenk techniques to exclude air and moisture from the reactions. The synthesis of TiO_2 was performed with benzyl alcohol and titanium tetrachloride ($TiCl_4$) under an inert atmosphere. Following literature procedures, both 4.5 nm and 8 nm diameter TiO_2 particles were synthesized by simple variations in the overall reaction procedure.[40] The synthesis of both Fe_3O_4 and ZnO were performed using benzyl alcohol and the corresponding metal acetate with the reaction mixtures being heated to a relatively low temperature of 200 °C.[39] The one pot synthesis techniques for MONPs allows for easy scale up of reactions without the loss from lower percent yields seen in multistep synthesis.

2.3 Polyoxometallates

Two different structural classes of polyoxometallates (POMs) were synthesized as reactive additives: Keggin and Dawson as seen in Figure 1.7. The syntheses were all able to be performed open to air but the Keggin structure POMs requiring a high pressure vessel, shown in Figure 2.2, for hetero-metal substitution. Synthetically the

POMs were the intermediate group in terms of affordability and ease of synthesis. POMs are made from relatively cheap starting materials and use simple synthetic techniques. The major drawback for use of POMs is due to the multiple step pathways resulting in lower overall yields when compared to one pot syntheses. This is especially true for the Dawson structure POMs. Figure 2.3 is a reaction flow chart for the synthesis of the Keggin structural class of POMs.

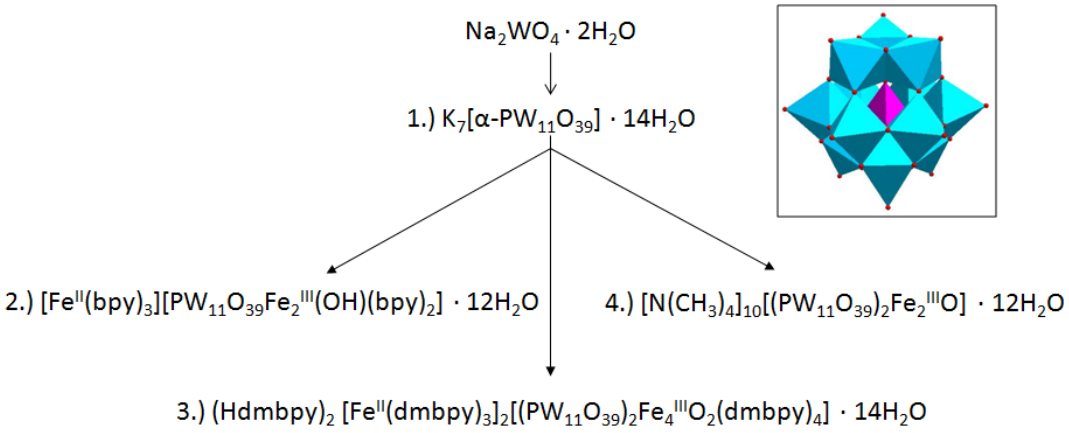

Figure 2.3: Reaction flow chart for Keggin structure POMs synthesized

As illustrated in Figure 2.3, POM synthesis starts with sodium tungstate dihydrate ($Na_2WO_4 \cdot 2H_2O$) which is reacted with 1 M phosphoric acid and 1 M acetic acid then refluxed followed by precipitation with potassium chloride.[59] The initial reaction creates the precursor Keggin cage structure which is then subjected to hetero-metal substitution. The Keggin precursor($K_7[\alpha\text{-}PW_{11}O_{39}] \cdot 14H_2O$), iron(III) sulfate and one of

the various organic molecules (2,2'-bipyridine (bpy), 5,5'-dimethyl-2,2'-bipyridine, and tetramethyl ammonium bromide) are then mixed in a beaker and placed into the bomb calorimeter for hydrothermal syntheses reactions under an air atmosphere resulting in the Keggin substituted products.[46]

The Dawson cage structure POMs follow a more elaborate reaction scheme as shown in Figure 2.4. The Dawson cage precursor requires more refinement before hetero-metal substitution.

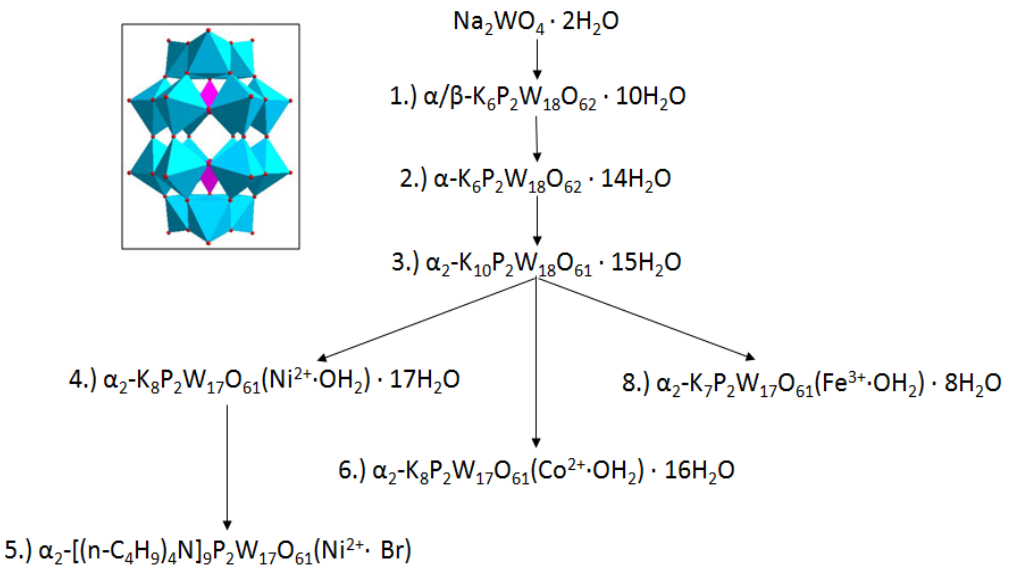

Figure 2.4: Reaction flow for the Dawson structure POMs synthesized

The first step in creating a Dawson structure reacts $Na_2WO_4 \cdot 2H_2O$ with concentrated phosphoric acid followed by refluxing overnight. The basic Dawson cage structure was precipitated with potassium chloride. The mixed structural isomer product is then

purified over the next two steps using basic solutions of potassium bicarbonate to isolate the pure alpha-2 isomer. Isomers of polyoxometallates are simple rotations of three of the tungsten octahedrons while maintaining all other positions. The different isomers allow different spacing from those shown in Figure 1.8. Purification and isolation of the alpha-2 isomer also allows hetero-metal substitution to take place at the same site for every substitution. Once the pure alpha-2 isomer is isolated, the hetero-metal substitutions involves simple reactions of α_2-$K_{10}P_2W_{17}O_{61}\cdot 15H_2O$ with the corresponding metal nitrate followed by precipitation with potassium chloride and recrystallization from water.[45]

The major drawback to utilization of POMs as reactive additives would be the multistep synthesis required for hetero-metal substitution. The multistep synthesis lowers total yield and increases the relative cost of the POMs. The advantage of using POMs as reactive additives is that with one precursor, multiple hetero-metal substitutions can be performed in one step reactions making multiple transition metal centers available as potential candidates for use in a self-decontamination surface.

2.4 Metal Functionalized Cyclodextrins

Cyclodextrins (CDs) offer the possibility of a reactive additive based upon the unique characteristics of the overall chemical structure of the macrocycles.[51] The ability to modify the cyclodextrin structures has also been demonstrated in the literature with both primary and secondary interfaces being modified.[52-57] The cyclodextrin additives proved to be the most difficult to synthesize, but they are relatively inexpensive for use

in reactive coatings. The goal of the research was to selectively functionalize the secondary interface with transition metals in order to create a reactive ring around the hydrophobic cavity in which the organic contaminants would reside. In order to isolate the secondary hydroxyl groups of the cyclodextrins a protecting group needed to be attached to the primary hydroxyl groups. Literature procedures outlined the protection of the primary hydroxyl groups for each commercially available cyclodextrin by using tert-butyl dimethylsilylchloride (TBDMSiCl).[52-54] Figure 2.5 shows a basic reaction scheme for the protection of the primary hydroxyl groups of β-CD.

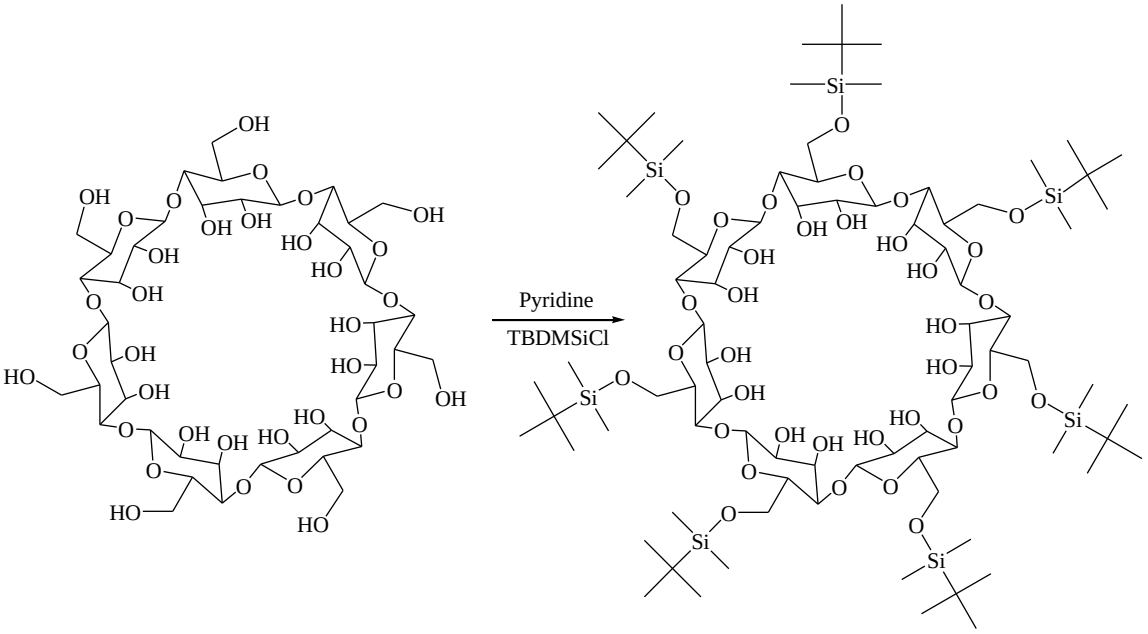

Figure 2.5: Reaction scheme for the protection of the primary hydroxyl groups on β-CD

The protection of β and γ-CD involve pyridine as the solvent and TBDMSiCl as is shown in the reaction scheme shown in Figure 2.5. The reactions are generally run for one to

two days and then isolated by precipitation with ice water and isolated by vacuum filtration. The protection of α-CD was performed in N,N-dimethylformamide (DMF) as the solvent with imidazole as a base mixed with TBDMSiCl. The final product was precipitated with ice water and isolated by vacuum filtration in the same process used for β and γ-CD.[52-54]

The literature shows that the reactions of transition metal chlorides produced complexes through adjacent oxygen atoms of a single glucose ligand after the hydroxyl groups were deprotonated via sodium adducts.[60-62] After the primary hydroxyl groups were protected the secondary hydroxyl groups were then reacted with transition metal chlorides in similar fashion to the way individual glucose units were reacted with transition metal chlorides. Based upon the structural characteristics of the cyclodextrin molecules and the stoichiometry of the reactions, the products of the CD based reactions should result in the products shown in Figure 2.6.

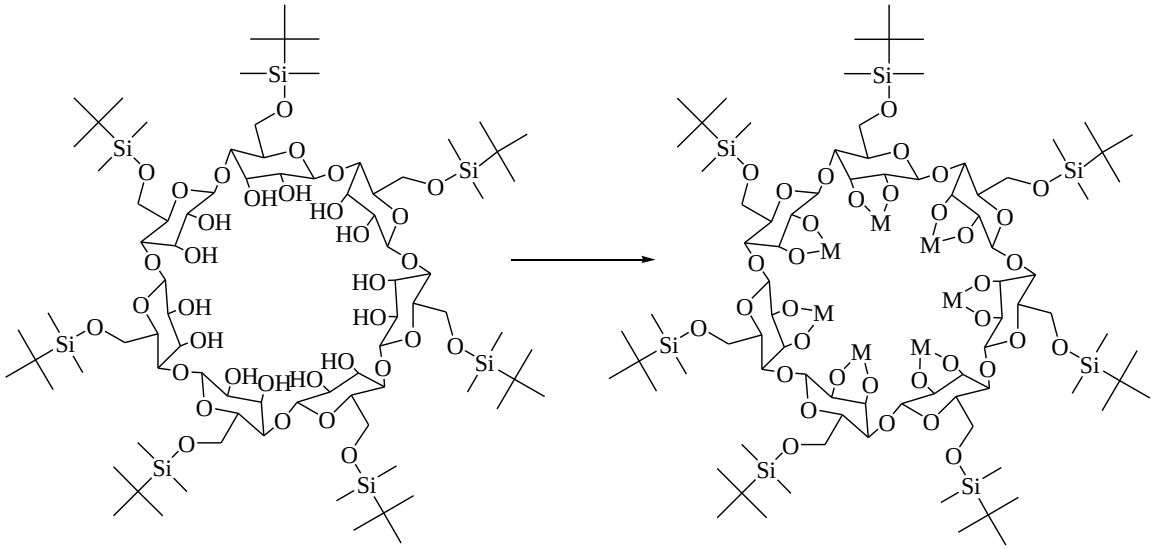

Figure 2.6: Reaction scheme of protected β-CD with transition metal chlorides

Three different reaction procedures were utilized in reacting the four different transition metal chlorides with the protected cyclodextrins. The reactions of titanium tetrachloride ($TiCl_4$) with protected cyclodextrins were performed in chloroform under an inert atmosphere using standard Schlenk line techniques. The protected cyclodextrins were dissolved in chloroform and then liquid $TiCl_4$ was added to the reaction vessel to form a clear yellow solution which was allowed to react for approximately two days. The clear yellow solutions evolved into white cloudy solutions over the course of the reaction and the products were isolated by removal of the solvent under vacuum. The reactions of iron(III) chloride and cobalt(II) chloride hexahydrate with protected cyclodextrins were performed in tetrahydrofuran (THF) with sodium hydride under an inert atmosphere in a three neck flask using standard Schlenk techniques. The protected cyclodextrins were dissolved in THF and then solid

sodium hydride was added to the solution and allowed to react for 30 minutes. Next, addition of the transition metal chloride was performed and the solutions were allowed to react for two to three days. Each product was isolated by evaporation of the solvent under vacuum using a rotary evaporator. The reactions of nickel(II) chloride ($NiCl_2$) with protected cyclodextrins were performed in N,N-dimethylformamide (DMF) with sodium hydride under an inert atmosphere in a three neck flask using standard Schlenk techniques. The protected cyclodextrins were dissolved in DMF followed by addition of sodium hydride which was allowed to react for 30 minutes. Next, addition of the $NiCl_2$ was performed and the solutions were allowed to react for two to three days. The solvent was then reduced under vacuum using a rotary evaporator followed by centrifugation of the remaining solution to isolate the solid.

2.5 Glass Transition Temperature

The modification of MIL-PRF-85285 involves changing the chemical make-up of the coating and could mean a change in the physical properties exhibited by the cured coating. The glass transition temperature (T_g) was determined for each modified coating as well as the unmodified MIL-PRF-85285 control coating to test for changes in T_g upon addition of additives. The glass transition temperature is the temperature at which a polymer transitions from an amorphous state to a crystalline state. Significant changes in the T_g values would indicate that the cured coating could be harder or softer than the initial MIL-PRF-85285 control coating meaning a change in the functional temperature range and durability of the coating. MIL-PRF-85285 has a specific

operational temperature range of -50 to 120 °C which cannot be modified significantly in order to stay within the military specifications. When a polymer is at a temperature above T_g, the polymer becomes elastic and can be formed to specific shapes. When the polymer is at a temperature below T_g, the polymer becomes hard and brittle making the coating less resistant to cracking under stress.[63] The current research is focused on the modification of coating systems with reactive additives toward CWA degradation. However, any modification to MIL-PRF-85285 needs to modify the reactivity toward CWAs and maintain T_g to keep the functional temperature range unchanged. The glass transition temperature for each coating was determined using differential scanning calorimetry (DSC). DSC experiments apply heat and maintain equal temperature to both a sample (coating) and a reference (air). DSC plots the heat flow into the sample vs. the temperature. A typical DSC plot is shown in Figure 2.7.

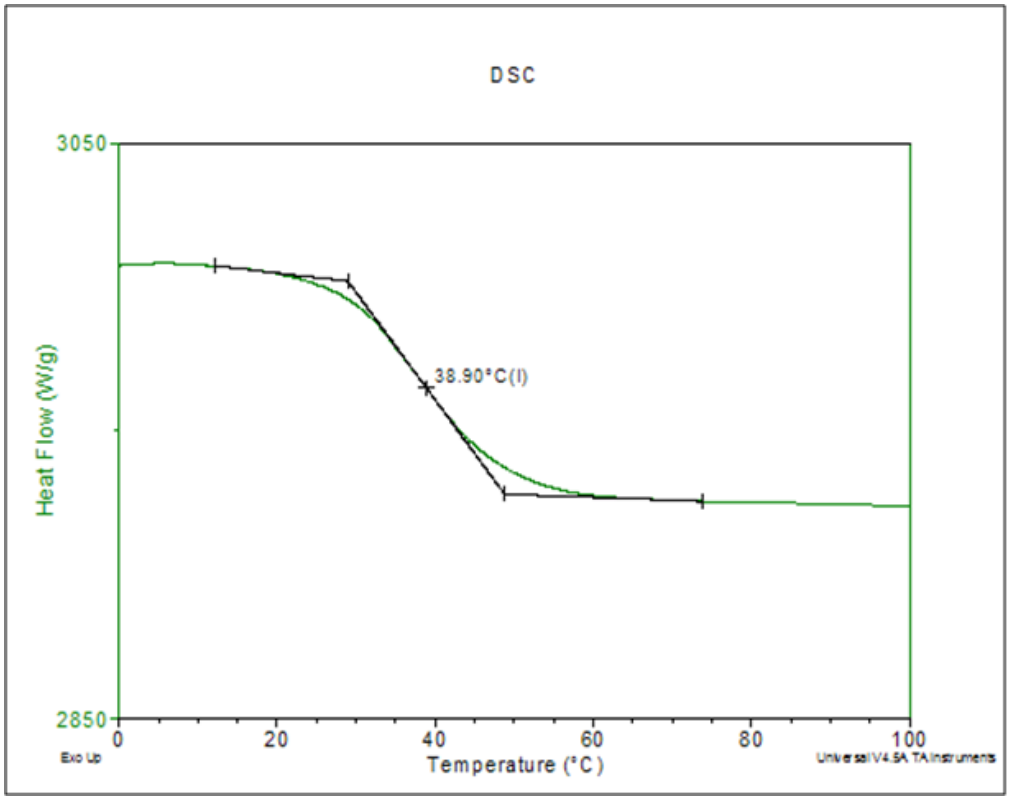

Figure 2.7: Example of a differential scanning calorimetry plot of heat flow vs. temperature

The heat flow for each sample is determined by the difference in the heat absorption of the sample (coating) and a reference (air). The inflection point of the curve seen in Figure 2.7 is the glass transition temperature (T_g) for the examined sample.

2.6 Contact Angle Analysis

The second important coating characterization test is contact angle analysis. Contact angle analysis provides information about how liquids will interact when deposited on the coated surfaces.[22] Every liquid has a certain surface tension and when the liquid is applied to a surface, the liquid will either bead up or spread out based upon the surface-liquid interface interaction. The contact angle measurements provide data

for determining an approximation of the coating surface free energy using the Owens/Wendt method. The Owens/Wendt method utilizes Equation 2.1 to approximate the surface free energy by relating the measured contact angle of a solvent on the surface and surface tension properties of the liquid.[21]

$$1 + cos\theta = 2\sqrt{\gamma_s^d}\left(\frac{\sqrt{\gamma_l^d}}{\gamma_{lv}}\right) + 2\sqrt{\gamma_s^h}\left(\frac{\sqrt{\gamma_l^h}}{\gamma_{lv}}\right) \qquad \text{Equation (2.1)}$$

Table 2.1 gives a breakdown of the variables in Equation 2.1 used in determining the approximate surface free energies of the control and modified coatings.[21]

Table 2.1: Definition of variables for Equation 2.1

Equation 2.1 Variables	Definition
θ	Measured contact angle
γ_s^d	Surface Diffusion Force
γ_s^h	Surface Hydrogen Bonding/ Dipole-Dipole Forces
γ_l^d	Liquid Diffusion Force
γ_l^h	Liquid Hydrogen Bonding/Dipole-Dipole Forces
γ_{lv}	Liquid Surface Energy

The measured contact angle (θ) and the surface tension data shown in Table 2.2 for the two solvents, water and diiodomethane, provide two equations to solve for the values of the two force components of the surface, γ_s^d and γ_s^h, from Equation 2.1.

Table 2.2: Surface tension data for water and diiodomethane

Liquid (20 °C)	γ_l^d (dynes/cm)	γ_l^h (dynes/cm)	γ_{lv} (dynes/cm)
Water	21.8	51	72.8
Diiodomethane	50.8	0	50.8

The sum of the two force components (γ_s^d and γ_s^h) is an approximation of the surface free energy for the coatings. Surface free energy approximations were determined for each of the modified coatings as well as the control coating to assess if the addition of reactive additives significantly changed the surface energy approximation. Any major change in the surface free energy approximation will change how different liquids interact with the surface upon deposition. Surface free energies for the modified coatings would ideally be unchanged due to the specification set by the military for MIL-PRF-85285.

Chapter 3 : Experimental

3.1 Synthesis

Three series of chemical compounds were synthesized in the effort towards the development of a continuous self-decontaminating surface: metal oxide nanoparticles, polyoxometallates and metal functionalized cyclodextrins. The metal oxide nanoparticles and cyclodextrin synthesis required the use of standard Schlenk techniques to maintain an inert atmosphere during reactions. Polyoxometallate syntheses were performed using standard bench top chemistry with utilization of a high pressure vessel for the Keggin structure POMs. All synthesized materials were isolated and used as described in the synthetic procedures. No further purification or assay for purity was performed for any of the compounds described herein.

3.1.1 Metal Oxide Nanoparticles

Three types of metal oxide nanoparticle were synthesized and tested as chemical decontamination paint additives: iron oxide (Fe_3O_4), zinc oxide (ZnO), and titanium dioxide (TiO_2). The chemicals iron(II) acetate 95%, zinc(II) acetate 99.99% and titanium tetrachloride 99.9% were purchased from Aldrich and used without further purification. Benzyl alcohol was purchased from Sigma-Aldrich was placed over 3 Å molecular sieves to remove any water.

*Note: The reactions forming Fe_sO_4 and ZnO were modified from the literature. Heating of the samples in the literature was performed using a microwave and

completed in minutes. Reactions reported herein were heated using a heating mantle and left to run overnight to ensure full reaction.

3.1.1.1 Synthesis of Fe_3O_4*

In a dry 100 mL Schlenk flask, 0.3480 g of iron(II) acetate was degassed and placed under an inert atmosphere of nitrogen. Dry benzyl alcohol, 10 mL, was added to the reaction flask via syringe and the mixture was then stirred. The reaction mixture was then heated to 200 °C and left to react overnight. The reaction was quenched by immersion of the reaction flask into and ice water bath and the product was isolated by centrifugation. The product was washed with ethanol and diethyl ether and dried in an oven overnight at 60 °C. [39] The dark brown solid, 0.080 g, was isolated in a 52% yield.

3.1.1.2 Synthesis of ZnO*

In a dry 100 mL Schlenk flask, 1.1017 g of zinc(II) acetate was degassed and placed under an inert atmosphere of nitrogen. Dry benzyl alcohol, 30 mL, was added to the reaction flask via syringe and the mixture was then stirred. The reaction mixture was then heated to 200 °C and left to react overnight. The reaction was quenched by immersion of the reaction flask into and ice water bath and the product was isolated by centrifugation. The product was washed with ethanol and diethyl ether and dried in an oven overnight at 60 °C. [39] The white solid, 0.3089 g, was isolated in a 63% yield.

3.1.1.3 Synthesis of 4.5 nm** TiO_2

In a dry three neck round bottom flask, 40 mL of benzyl alcohol was degassed and placed under an inert atmosphere of nitrogen. Titanium tetrachloride, 1 mL, was

added drop wise to the stirring benzyl alcohol. An initial bright yellow solution with a red precipitate formed upon the full addition of titanium tetrachloride. Upon further stirring the red precipitate dissolved into the yellow solution and was left to react at room temperature overnight. The reaction mixture was then heated to 40 °C for seven days after which a thick white suspension evolved. The white solid was isolated by centrifugation, washed with ethanol and dried open to air. [40] The solid was ground into a fine white powder with a mass of 0.7652 g which was 105% yield indicating an impurity.

**Note: Particle size is assumed based upon the procedure outlined in the literature.

3.1.1.4 Synthesis of 8 nm** TiO_2

A dry 100 mL flask was degassed and placed under an inert atmosphere of nitrogen. Dry benzyl alcohol, 5 mL, was added to the flask and stirred. Following the addition of the benzyl alcohol, the titanium tetrachloride, 0.5 mL, was added drop wise to give a yellow solution which was stirred while heated to 150 °C and left to react overnight. The solution evolved to a thick yellow-white suspension which afforded a yellow-white solid when centrifuged and washed with ethanol. [40] The solid was allowed to dry open to air to produce a fine white powder and thick yellow putty. The putty was discarded and the powder was isolated and dried to give 0.0669 g for an overall 18% yield.

**Note: Particle size is assumed based upon the procedure outlined in the literature.

3.1.2 Polyoxometallates

Two cage structure families of polyoxometallates were utilized in the effort to create a continuous self-decontaminating surface: Keggin ($XM_{12}O_{40}^{n-}$) and Dawson ($X_2M_{18}O_{62}^{n-}$) where X = phosphorous (P) and M = tungsten (W). The chemicals sodium tungstate dihydrate and 2,2'-bipyridine were purchased from Strem Chemicals and used without further purification. Phosphoric acid, iron(III) sulfate, 5,5'-dimethyl-2,2'-bipyridine, and tetramethyl ammonium bromide, potassium hydroxide and bromine were purchased from Aldrich and used without further purification. Acetic acid, hydrochloric acid, dichloromethane, and sulfuric acid were purchased from EMD and were used without further purification. Potassium chloride was purchased from Mallinckrodt Chemicals and used without further purification. Potassium bicarbonate, cobalt(II) nitrate hexahydrate, iron(III) nitrate nonahydrate, nickel(II) nitrate hexahydrate were purchased from J. T. Baker and were used without further purification. Tetrabutyl ammonium bromide was purchased from TCI America and used without further purification. Acetonitrile was purchased from EM Science and used without further purification.

3.1.2.1 Synthesis of $K_7[\alpha\text{-}PW_{11}O_{39}]\cdot 14H_2O$

In a 50 mL round bottom flask, 7.2611 g of sodium tungstate dihydrate was dissolved in 12.2 mL of distilled water. The solution was stirred and 2 mL of 1 M phosphoric acid was added to the solution followed by 3.60 mL of 1 M acetic acid. The reaction vessel was fitted with a reflux condenser and the solution was refluxed for one

hour. After reflux, 2.4074 g of potassium chloride was added to the solution affording a fine precipitate.[59] The solution was placed in the refrigerator overnight and the white solid, 1.4913 g, was isolated by filtration for a 23.26% yield.

3.1.2.2 Synthesis of $[Fe^{II}(bpy)_3][PW_{11}O_{39}Fe_2^{III}(OH)(bpy)_2]\cdot 12H_2O$

In a 50 mL beaker, 0.5504 g of $K_7[\alpha\text{-}PW_{11}O_{39}]\cdot 14H_2O$, 0.1042 g of iron (III) sulfate, and 0.1368 g of 2,2'-bipyridine (bpy) were mixed in 6 mL of distilled water. The pH of the solution was determined and no further adjustment was required. The solution was mixed and the beaker was placed into a Parr Instrument Company bomb calorimeter and sealed for performing the hydrothermal reaction. The calorimeter was then placed in a sand bath and heated to 160 °C and left to react for 72 hours. After 72 hours the bomb calorimeter was removed from the sand bath and allowed to cool to room temperature for 24 hours.[46] The dark red product, 0.1714 g, was isolated by filtration and washed with ethanol and dried open to air to give a 27.61% yield.

3.1.2.3 Synthesis of $(Hdmbpy)_2[Fe^{II}(dmbpy)_3]_2[(PW_{11}O_{39})_2Fe_4^{III}O_2(dmbpy)_4]\cdot 14H_2O$

In a 50 mL beaker, 0.5508 g of $K_7[\alpha\text{-}PW_{11}O_{39}]\cdot 14H_2O$, 0.1038 g iron(III) sulfate, and 0.1411 g of 5,5'-dimethyl-2,2'-bipyridine were mixed in 6 mL of distilled water. The pH of the solution was determined and no further adjustment was required. The solution was mixed and the beaker was placed into a Parr Instrument Company bomb calorimeter and sealed for performing the hydrothermal reaction. The calorimeter was then placed in a sand bath and heated to 160 °C and left to react for 72 hours. After 72 hours the bomb calorimeter was removed from the sand bath and allowed to cool to

room temperature for 48 hours.[46] The dark red solid, 0.4514 g, was scraped from the beaker and washed with ethanol and dried open to air for a 71.46% yield.

3.1.2.4 Synthesis of $[N(CH_3)_4]_{10}[(PW_{11}O_{39})_2Fe_2^{III}O]\cdot 12H_2O$

In a 50 mL beaker, 0.3869 g of $K_7[\alpha\text{-}PW_{11}O_{39}]\cdot 14H_2O$, 0.0729 g of iron(III) sulfate, and 0.0955 g of tetramethyl ammonium bromide were mixed in 4.5 mL of distilled water. The pH was tested and adjusted to 4 with a drop of 2 M potassium hydroxide. The solution was mixed and the beaker was placed into a Parr Instrument Company bomb calorimeter and sealed for performing the hydrothermal reaction. The calorimeter was then placed in a sand bath and heated to 160 °C and left to react for 72 hours. After 72 hours the bomb calorimeter was removed from the sand bath and allowed to cool to room temperature for 48 hours. The yellow solid, 0.3965 g, was scraped from the beaker and washed with ethanol and dried to give 101% yield.[46]

3.1.2.5 Synthesis of $\alpha/\beta\text{-}K_6P_2W_{18}O_{62}\cdot 10H_2O$

In a 1000 mL Erlenmeyer flask, 100.0535 g of sodium tungstate dihydrate was dissolved in 350 mL of 90 °C distilled water. Once the entire amount of solid was dissolved, 150 mL of 85% phosphoric acid was added over 30 minutes during which time the solution evolved into a light green color. Once all of the acid was added, the solution was refluxed overnight. After the solution was refluxed overnight 100 g of potassium chloride was added to afford a fine white precipitate. The white solid was isolated by filtration and the filtrate was boiled and allowed to cool to 5 °C and a second amount of white solid was isolated by filtration. The two amounts of isolated solid were

then recrystallized from boiling water and the solution was cooled to 5 °C overnight.[45] The light green-white solid, 37.49 g, was isolated by filtration and washed with distilled water followed by ethanol and then diethyl ether to give a 45.98% yield.

3.1.2.6 Synthesis of α-$K_6P_2W_{18}O_{62}\cdot 14H_2O$

In a 1000 mL Erlenmeyer flask, 37.1442 g of α/β-$K_6P_2W_{18}O_{62}\cdot 10H_2O$ was dissolved in 135 mL of 80 °C distilled water forming a light green solution. One drop of bromine was added to the solution changing the solutions color from a light green to a light yellow color. The solution was stirred while 212 mL of 1 M potassium bicarbonate was added over five minutes causing a white precipitate to form. After the potassium bicarbonate was added, the solution was left to react for 30 minutes during which time the precipitate dissolved forming a clear solution. Next, 80 mL of 6 M hydrochloric acid was added to the mixture over a ten minute period. The solution turned yellow and a fine white precipitate evolved. The solution was filtered to remove the white precipitate and 53.0222 g of solid potassium chloride was added to the filtrate and the solution was allowed to cool to 5 °C overnight. The product was isolated and recrystallized in water that was then cooled to 5 °C.[45] The final white solid, 11.4107 g, was isolated by filtration for a 29.5% yield.

3.1.2.7 Synthesis of α_2-$K_{10}P_2W_{17}O_{61}\cdot 15H_2O$

In a 100 mL Erlenmeyer flask, 11.4107 g of α-$K_6P_2W_{18}O_{62}\cdot 14H_2O$ was added to 25.1 mL of 40 °C distilled water and stirred creating a light green solution. After the formation of the light green solution 42.2 mL of 1 M potassium bicarbonate was added

slowly to create a white solution that was left to react for 30 minutes. The white solid was isolated by filtration followed by recrystallization from 20 mL of boiling distilled water. [45] The white solid was washed with water, ethanol, diethyl ether and then dried under vacuum for eight hours to give 7.8856 g of final product giving a 68.3% yield.

3.1.2.8 Synthesis of α_2-$K_8P_2W_{17}O_{61}(Co^{2+}\cdot OH_2)\cdot 16H_2O$

In a small Schlenk flask, 0.5192 g of α_2-$K_{10}P_2W_{17}O_{61}\cdot 15H_2O$ was dissolved in 2.0 mL of 90 °C of distilled water. Next, a solution of cobalt(II) nitrate hexahydrate (0.0339 g dissolved in 0.4 mL of distilled water) was added to the reaction vessel creating a dark red solution. The solution was left to stir for for 15 minutes after which 0.3084 g of potassium chloride was added and the solution allowed to cool to room temperature. The solution was then placed into the refrigerator and cooled to 5 °C for one hour.[45] A red brown solid was isolated and the solid was recrystallized from boiling water twice and isolated by filtration and washed with distilled water to give 0.2719 g for a 52.2% yield.

3.1.2.9 Synthesis of α_2-$K_7P_2W_{17}O_{61}(Fe^{3+}\cdot OH_2)\cdot 8H_2O$

In a small Schlenk flask, 1.0101 g of α_2-$K_{10}P_2W_{17}O_{61}\cdot 15H_2O$ was dissolved in 3 mL of 90 °C distilled water. Next, a solution of iron(III) nitrate nonahydrate (0.0888 g dissolved in 0.4 mL of distilled water) was added to the reaction vessel creating a dark yellow-orange solution. Bromine, three drops, was added to the reaction solution to ensure full oxidation. Following the addition of bromine, the solution was boiled and the volume was reduced from 3 mL to 2 mL. The final solution was filtered and 0.5005 g

of potassium chloride was added to the filtrate. The solution was heated to 60 °C until the solution was homogenized. The solution was then allowed to cool to room temperature and then cooled to 5 °C in a refrigerator overnight after which the crude yellow solid was isolated by filtration. The crude product was recrystallized from boiling water and the final product was isolated by filtration. The final product was washed with distilled water and dried under vacuum overnight.[45] The light yellow solid, 0.6367 g, was isolated to give a 64.35% yield.

3.1.2.10 Synthesis of α-$K_8P_2W_{17}O_{61}(Ni^{2+}\cdot OH_2)\cdot 17H_2O$

In a 5 mL beaker, 0.5056 g of α_2-$K_{10}P_2W_{17}O_{61}\cdot 15H_2O$ was dissolved in 1 mL of 90 °C of distilled water. Next, a solution of nickel(II) nitrate hexahydrate (0.0350 g dissolved in 0.4 mL of distilled water) was added to the reaction vessel creating a bright green solution which was stirred for 15 minutes. The solution was then cooled for 5 °C in a refrigerator overnight to afford a bright green solid which was isolated by filtration and recrystallized from boiling distilled water. The final green solid, 0.2326 g, was isolated by filtration and washed with distilled water.[45] The solid was dried under vacuum overnight to give a 45.61% yield.

3.1.2.11 Synthesis of α_2-$[(n\text{-}C_4H_9)_4N]_9P_2W_{17}O_{61}(Ni^{2+}\cdot Br)$

In a 50 mL round bottom flask, 0.2296 g of α-$K_8P_2W_{17}O_{61}(Ni^{2+}\cdot OH_2)\cdot 17H_2O$ was dissolved in 12 mL of distilled water forming a light green solution. Next, tetrabutyl ammonium bromide, 0.1216 g, followed by two drops of 0.18 M sulfuric acid was added to the mixture and a cloudy white solution was formed. Dichloromethane, 11.50 mL,

was then added to the mixture and stirred for five minutes. After five minutes the solution was allowed to settle into two layers, an aqueous milky white layer and an organic light yellow layer. The organic layer was isolated and the solvent was removed under vacuum to yield a yellow solid. The solid was then dissolved in acetonitrile to give a yellow oil which was then triturated with diethyl ether to afford a yellow paste.[45] Upon further addition of ether the yellow paste evolved into a fine yellow powder that was isolated and dried under vacuum to give 0.1712 g a 55.64% yield.

3.1.3 Metal Functionalized Cyclodextrins

The three commercially available cyclodextrins alpha, beta and gamma were modified with transition metals to give three series of cyclodextrin products. Each cyclodextrin was modified with titanium, nickel, cobalt and iron on the secondary interface in hopes of creating a reactive additive with the ability to form inclusion complexes with the target contaminants. The chemicals alpha cyclodextrin (α-CD) and gamma cyclodextrin (γ-CD) were purchased from TCI and were stored in an oven to remove any excess water. Beta cyclodextrin (β-CD) was purchased from TCI America and stored in an oven to remove any excess water. Anhydrous dimethylformamide (DMF), iron(III) chloride, and methanol were purchased from Sigma-Aldrich and used without further purification. Imidazole, pyridine, and tetrahydrofuran (THF) were purchased from EMD. The pyridine and the THF were both distilled to ensure no excess water was present in the solvents. Tert-butyl dimethylsilylchloride was purchased from Arcos Organics and used without further purification. Nickel(II) chloride and cobalt(II)

chloride hexahydrate were purchased from Aldrich and used without further purification. Sodium hydride was purchased from Alfa Aesar and was washed with hexanes before use in reactions. Ammonium fluoride was purchased from J.T. Baker and used without further purification.

***Note: The percent yields for the reactions of the transition metal chlorides with protected cyclodextrins are not reported herein because the true chemical structure of the products is not known.

3.1.3.1 Synthesis of Protected Alpha Cyclodextrin

A dry 250 mL three neck flask was degassed and placed under an inert atmosphere of argon. Once under inert atmosphere, 80 mL of anhydrous dimethylformamide (DMF) was added to the flask using a syringe. Utilizing the side neck of the flask solid alpha cyclodextrin (α-CD), 3.471 g, and imidazole, 3.3321 g, was dissolved in the DMF to afford a clear solution. In a separate round bottom flask, 3.563 g of tert-butyl dimethylsilylchloride was dissolved in 70 mL of anhydrous DMF to give a clear solution which was added to the α-CD reaction solution. The final solution was allowed to react six days after which the solution remained clear. The solution was poured over ice water to produce a fluffy white precipitate which was isolated by vacuum filtration.[52] The white solid was washed with cold distilled water and dried in an oven at 80 °C for 2 days giving 5.0871 g of product for an 86% yield.

3.1.3.2 Synthesis of Protected Beta Cyclodextrin

In a dry 250 mL three neck flask 9.217 g of beta cyclodextrin was degassed and placed under an inert atmosphere of argon. Next, 100 mL of distilled pyridine was added to the flask and stirred to produce a clear solution. In a separate flask, 9.98 g of tert-butyl dimethylsilylchloride was dissolved in 80 mL of distilled pyridine. The solution of tert-butyl dimethylsilylchloride was then added to the reaction flask using a syringe to give a clear solution. The reaction vessel was then placed in an ice bath and left to react for two hours. The reaction vessel was then removed from the ice bath and the solution was allowed to come up to room temperature and allowed to react for two days. The reaction solution was then poured over ice water to produce a fluffy white precipitate which was isolated by vacuum filtration.[54] The product was then washed with cold water and dried in an oven at 80 °C for one day to give 14.859 g of product for a 94.6% yield.

3.1.3.3 Synthesis of Protected Gamma Cyclodextrin

A dry three neck flask was degassed and placed under inert atmosphere of argon. Pyridine, 125 mL, was added to the flask and stirred rapidly. Next 6.4046 g of gamma cyclodextrin (γ-CD) was added to the reaction flask and stirred to give a clear solution. In a separate flask 6.5716 g of tert-butyl dimethylsilylchloride was dissolved in 60 mL of distilled pyridine. The solution of tert-butyl dimethylsilylchloride was then added to the reaction flask using a syringe to give a clear solution. The reaction vessel was then placed in an ice bath and allowed to react for two hours. The reaction vessel

was then removed from the ice bath and the solution was allowed to come up to room temperature and then allowed react for two days. The reaction solution was then poured over ice water to produce a fluffy white precipitate which was isolated by vacuum filtration.[54] The product was then washed with cold water and left to dry open to air followed by drying in an oven at 80 °C for one day to give 9.929 g of product for a 90.9% yield.

3.1.3.4 Reaction of Titanium Tetrachloride and Protected α-CD***

In a dry 50 mL Schlenk flask, 0.4275 g of protected α-CD was degassed and placed under an inert atmosphere of argon. Next, 20 mL of chloroform was added to the reaction vessel using a syringe and stirred to afford a clear solution. After the solid was completely dissolved, 0.200 mL of titanium tetrachloride ($TiCl_4$) was added slowly to the reaction solution with a syringe to afford a clear yellow solution. The reaction was left to react at room temperature for three days during which time the solution evolved to a milky white solution with a hint of yellow. The product was isolated by removal of the solvent under vacuum to yield 0.4964 g of a white-yellow solid.

3.1.3.5 Reaction of Titanium Tetrachloride and Protected β-CD***

In a dry 50 mL Schlenk flask, 0.3196 g of protected β-CD was degassed and placed under an inert atmosphere of argon. Next, 20 mL of chloroform was added to the reaction vessel using a syringe and stirred to afford a clear solution. After the solid was completely dissolved, 0.145 mL of titanium tetrachloride was added slowly to the reaction solution with a syringe to afford a clear yellow solution. The reaction was left

to react at room temperature for two days during which time the solution evolved to a milky white solution with a hint of yellow. The product was isolated by removal of the solvent under vacuum to yield 0.4153 g of a white-yellow solid.

3.1.3.6 Reaction of Titanium Tetrachloride and Protected γ-CD***

In a dry 50 mL Schlenk flask, 0.5183 g of protected γ-CD was degassed and placed under an inert atmosphere of argon. Next, 20 mL of chloroform was added to the reaction vessel using a syringe and stirred to afford a clear solution. After the solid was completely dissolved, 0.220 mL of titanium tetrachloride was added slowly to the reaction solution with a syringe to afford a clear yellow solution. The reaction was left to react at room temperature for two days during which time the solution evolved to a milky white solution with a hint of yellow. The product was isolated by removal of the solvent under vacuum to yield 0.6840 g of a white-yellow solid.

3.1.3.7 Reaction of Nickel(II) Chloride and Protected α-CD***

In a dry 250 mL three neck flask, 0.6020 g of protected α-CD was degassed and placed under and inert atmosphere of nitrogen. Next, 50 mL of anhydrous DMF was added to the reaction vessel with a syringe and stirred to form a clear solution. After the solid was dissolved, 0.5390 g of sodium hydride was added to the reaction flask and allowed to react for 30 minutes. After the addition of sodium hydride, the solution turned cloudy white and thick foam formed above the solution which remained for the rest of the experiment. After thirty minutes had elapsed, 0.2894 g of nickel(II) chloride was added to the reaction flask, changing the color of the solution to a light orange

cloudy color. The solution was allowed to react for two days during which the solution evolved into a pale green cloudy color. The reaction was then opened to air, transferred to a 500 mL round bottom flask and the reaction solution quenched with excess methanol to ensure that the remaining sodium hydride was consumed. The solvent was reduced to 100 mL using a rotary evaporator, and then transferred to centrifuge tubes for isolation of the solid by centrifugation. The final light green solid was washed with distilled water and allowed to dry open to air. The solid was then stored in an oven at 80 °C to completely dry giving a yield of 0.4892 g of pale green product.

3.1.3.8 Reaction of Nickel(II) Chloride and Protected β-CD***

In a dry 100 mL three neck flask, 0.5128 g of protected β-CD was degassed and placed under and inert atmosphere of nitrogen. Next, 20 mL of anhydrous DMF was added to the reaction vessel with a syringe and stirred to form a clear solution. After the solid was dissolved, 0.4837 g of sodium hydride was added to the reaction flask and allowed to react for 30 minutes. After the addition of sodium hydride, the solution turned cloudy white and thick foam formed above the solution which remained for the rest of the experiment. After thirty minutes had elapsed 0.2485 g of nickel(II) chloride was added to the reaction flask, changing the color of the solution to a light orange cloudy color. The solution was allowed to react for two days during which the solution evolved into a pale green cloudy color. The reaction was then opened to air, transferred to a 250 mL round bottom flask and the reaction solution quenched with excess methanol to ensure that the remaining sodium hydride was consumed. The solvent was

reduced to 100 mL using a rotary evaporator then transferred to centrifuge tubes and the solid was isolated by centrifugation. The final light green solid was washed with distilled water and allowed to dry open to air. The final solid was then stored in an oven at 80 °C to completely dry for a yield of 0.7954 g of pale green product.

3.1.3.9 Reaction of Nickel(II) Chloride and Protected γ-CD***

In a dry 100 mL three neck flask, 0.6519 g of protected γ -CD was degassed and placed under and inert atmosphere of nitrogen. Next, 50 mL of anhydrous DMF was added to the reaction vessel with a syringe and stirred to form a clear solution. After the solid was dissolved, 0.5897 g of sodium hydride was added to the reaction flask and allowed to react for 30 minutes. After the addition of sodium hydride the solution turned cloudy white and thick foam formed above the solution which remained for the rest of the experiment. After thirty minutes had elapsed, 0.3099 g of nickel(II) chloride was added to the reaction flask, changing the color of the solution to a light orange cloudy color. The solution was allowed to react for three days during which the solution evolved into a pale green cloudy color. The reaction was then opened to air, transferred to a 500 mL round bottom flask and the reaction solution quenched with excess methanol to ensure that the remaining sodium hydride was consumed. The solvent was reduced to 100 mL using a rotary evaporator, and then transferred to centrifuge tubes and the solid was isolated by centrifugation. The final light green solid was washed with distilled water and allowed to dry open to air. The final solid was then stored in an oven at 80 °C to completely dry for a yield of 0.5546 g of a pale green product.

3.1.3.10 Reaction of Iron(III) Chloride and Protected α-CD***

In a dry 100 mL three neck flask, 30 mL of distilled tetrahydrofuran (THF) was added via syringe and placed under an inert atmosphere of nitrogen. Protected α-CD, 0.5197 g, was then added to the reaction flask and dissolved to form a clear solution upon stirring. Sodium hydride, 0.4655 g, was added to the reaction mixture forming a white cloudy solution and was allowed to react for 30 minutes. After 30 minutes, 0.3072 g of iron(III) chloride was added to the reaction mixture giving a yellow-brown colored solution which was allowed to react for two days. After two days the reaction solution evolved to an olive green-brown solution which was then exposed to air and quenched with excess methanol. The solution evolved from an olive green-brown color to a dark brown solution which was then transferred to a 250 mL round bottom flask and the solvent was removed with a rotary evaporator. The rust brown solid product, 1.2080 g, was isolated and stored in an oven at 80 °C.

3.1.3.11 Reaction of Iron(III) Chloride and Protected β-CD***

In a dry 100 mL three neck flask, 30 mL of distilled THF was added via syringe and placed under an inert atmosphere of nitrogen. Protected β-CD, 0.7072 g, was then added to the reaction flask and dissolved to form a clear solution upon stirring. Sodium hydride, 0.6326 g, was added to the reaction mixture forming a white cloudy solution and was allowed to react for 30 minutes. After 30 minutes, 0.4203 g of iron(III) chloride was added to the reaction mixture giving a yellow-brown colored solution which was allowed to react for two days. After two days, the reaction solution evolved to an olive

green-brown solution which was then exposed to air and quenched with excess methanol. The solution evolved from an olive green-brown color to a dark brown solution which was then transferred to a 250 mL round bottom flask and the solvent was removed with a rotary evaporator. The rust brown solid product, 0.2263 g, was isolated and stored in an oven at 80 °C.

3.1.3.12 Reaction of Iron(III) Chloride and Protected γ-CD***

In a dry 100 mL three neck flask, 30 mL of distilled THF was added via syringe and placed under an inert atmosphere of nitrogen. Protected γ-CD, 0.6885 g, was then added to the reaction flask and dissolved to form a clear solution upon stirring. Sodium hydride, 0.6284 g, was added to the reaction mixture forming a white cloudy solution and was allowed to react for 30 minutes. After 30 minutes, 0.4457 g of iron(III) chloride was added to the reaction mixture giving a yellow-brown colored solution which was allowed to react for two days. After two days, the reaction solution evolved to an olive green-brown solution which was exposed to air and quenched with excess methanol. The solution evolved from an olive green-brown color to a dark brown solution which was then transferred to a 250 mL round bottom flask and the solvent was removed with rotary evaporator. The rust brown solid product, 1.6932 g, was isolated and stored in an oven at 80 °C.

3.1.3.13 Reaction of Cobalt(II) Chloride Hexahydrate and Protected α-CD***

In a dry 250 mL three neck flask, 30 mL of distilled THF was added via syringe and placed under an inert atmosphere of argon. Protected α-CD, 0.4090 g, was added to the

reaction flask and stirred to give a clear solution. Next, sodium hydride, 0.3876 g, was added to the reaction solution to give a milky white solution which was allowed to react for 30 minutes. After 30 minutes, cobalt(II) chloride hexahydrate, 0.3586 g, was added to the solution. Upon addition of the cobalt(II) chloride hexahydrate, the solution turned baby blue and released gas vigorously. The solution was then left to react overnight at room temperature. After overnight reaction, the solution had evolved into a dark blue-black solution which was then exposed to air and quenched with methanol to remove any excess sodium hydride. The solvent was then removed using a rotary evaporator to isolate the final product which was dried in an oven at 80 °C for 72 hours to yield 0.7616 g of a black solid.

3.1.3.14 Reaction of Cobalt(II) Chloride Hexahydrate and Protected β-CD***

In a dry 250 mL three neck flask, 30 mL of distilled THF was added via syringe and placed under an inert atmosphere of argon. Protected β-CD, 0.4508 g, was added to the reaction flask and stirred to give a clear solution. Next, sodium hydride, 0.4402 g, was added to the reaction solution to give a milky white solution which was allowed to react for 30 minutes. After 30 minutes, cobalt(II) chloride hexahydrate, 0.4188 g, was added to the solution. Upon addition of the cobalt(II) chloride hexahydrate, the solution turned baby blue and released gas vigorously. The solution was then left to react overnight at room temperature. After overnight reaction, the solution had evolved into a dark blue-black solution which was then exposed to air and quenched with methanol to remove any excess sodium hydride. The solvent was then removed using a rotary

evaporator to isolate the final product which was dried in an oven at 80 °C for 72 hours to yield 0.8108 g of a black solid.

3.1.3.15 Reaction of Cobalt(II) Chloride Hexahydrate and Protected γ-CD***

In a dry 250 mL three neck flask, 30 mL of distilled THF was added via syringe and placed under an inert atmosphere of argon. Protected γ-CD, 0.4329 g, was added to the reaction flask and stirred to give a clear solution. Next, sodium hydride, 0.3809 g, was added to the reaction solution to give a milky white solution which was allowed to react for 30 minutes. After 30 minutes, cobalt(II) chloride hexahydrate, 0.3833 g, was added to the solution. Upon addition of the cobalt(II) chloride hexahydrate, the solution turned baby blue and released gas vigorously. The solution was then left to react overnight at room temperature. After overnight reaction the solution had evolved into a dark blue-black solution which was then exposed to air and quenched with methanol to remove any excess sodium hydride. The solvent was then removed using a rotary evaporator to isolate the final product which was dried in an oven at 80 °C for 72 hours to yield 0.7638 g of a black solid.

3.2 Coatings Preparations

Commercially available paint, MIL-PRF-85285, manufactured by DEFT Inc. (Irvine, CA) was modified with synthesized additives in a 1% w/w ratio of additives to paint. MIL-PRF-85285 is a two component polyurethane and is mixed in a 3:1 ratio followed by enhancement with synthesized additives. The paint was mixed by both mechanical stirring and vortex mixing to ensure a completely uniform dispersion of synthesized

additives is achieved. The modified coatings were then applied to pre-cleaned aluminum sheets for decontamination challenges against CWA simulants. The application of the coatings to the desired substrate while maintaining uniform thickness was performed using a Dayton™ 4RR09 Air brush at 25 psi. The final coated substrates were allowed to cure under ambient conditions for a minimum of 24 hours prior to any surface experimentation. The coatings were approximately 4 mils or 100 µm thick for all prepared samples.

3.3 Decontamination Challenges

Decontamination experiments were performed in triplicates and the standard deviations were determined for each modified coating against the four CWA simulants: CEES, CEPS, Demeton-S and Malathion. The simulants CEES and CEPS were purchased from Sigma Aldrich and Demeton-S and Malathion were purchased from Chem Service and were use without further purification. Four coated circular discs, 2 cm^2, were cut out and used as model surfaces for the decontamination challenges. On each disc a 0.5 µL aliquot of CWA simulant was applied and the disc was placed into a test tube which was then sealed. Two control samples were also created for each simulant tested. The control samples include an empty test tube loaded with 0.5 µL of CWA simulant and a test tube loaded with a control coating (paint with no additive) with 0.5 µL of CWA simulant applied to the surface. The simulants were allowed to reside on the coated surfaces or in the empty tube for 24 hours in the absence of light. Each sample following the residence time was then extracted with a 1 mL aliquot of acetonitrile

which was vortexed in the sample tube for 20 seconds. After being thoroughly mixed, each sample was collected in a 1 mL syringe and then filtered through a 0.2 µm syringe filter into a 1.5 mL GC/MS vial equipped with Teflon septa. Each sample was then subjected to GC/MS analysis for percent reduction of CWA simulants.

3.4 Gas Chromatography/Mass Spectrometry Analysis

Gas chromatography/mass spectrometry (GC/MS) analysis was utilized to monitor the simulant decontamination challenge experiments. The GC/MS instrumentation utilized was an Agilent 7890A gas chromatograph coupled with an Agilent 5975C mass selective detector equipped with an Agilent 7693A autoinjector. The gas chromatograph was equipped with an Agilent HP-5MS (5% phenyl) methylpolysiloxane film column. The carrier gas was helium and was run at a flow rate of 1 mL/min. The injection volume was 1 µL and a split injection was used at a ratio of 20:1. The temperature program starts at an initial temperature of 100 °C for one minute followed by a temperature ramp of 25 °C per minute to 130 °C. After 130 °C is reached, the temperature was ramped at 15 °C per minute to 250 °C followed by a one minute temperature plateau at 300 °C for one minute after the completion of the run. The injector temperature was set to 300 °C with the source temperature set at 230 °C. The mass selective detector was operating in electron ionization mode set to scan a mass range of 20 to 350 *m/z* with the MS quad temperature set at 150 °C.

3.5 Coatings Characterization

Each individual modified coatings system needed to maintain the initial coatings properties outlined by DEFT Inc. for MIL-PRF-85285. The modified coatings were therefore tested for changes in the glass transition temperature (T_g) and the surface free energy. Significant changes to either T_g or the surface free energy would mean the modified coating system would fall outside the operational parameters and could not be employed. The glass transition temperature was determined by Differential Scanning Calorimetry and the surface free energy was determined by Contact Angle Analysis.

3.5.1 Differential Scanning Calorimetry

The glass transition temperatures were determined using a TA Instruments Q20 Differential Scanning Calorimeter. The instrument was placed under an inert atmosphere of nitrogen at a flow rate of 50 mL/min. The instrument was equilibrated at -90 °C followed by a temperature ramp to 150 °C at a rate of 20 °C/min. The temperature ramp was repeated and the second scan was utilized for the determination of the glass transition temperature. The repetition was performed on all samples to remove any possible contaminants as well as to demonstrate the reversibility of the process. The coatings tested were first removed from the aluminum substrate and then subjected to DCS analysis. The glass transition temperature values for each modified coating were determined using Universal Analysis 2000 software by finding the inflection point of the heat capacity shift.

3.5.2 Contact Angle Analysis

Contact angle analysis and surface free energy approximations were performed with an AST Products Inc. VCA 2500 video contact angle system using the sessile drop technique. The sessile drop technique measures the contact angle of a static drop of liquid deposited on a flat surface. The drops of liquid were deposited on the surface by contact of a pendant drop on a syringe with the surface of interest. High resolution images of the drops of liquid on the surface were captured 3 seconds after the application of the probe solvent. Two probe solvents were utilized in the determination of the contact angle and the calculated surface free energy approximation: diiodomethand and triple distilled water. The contact angles were measured using VCA OptimaXE software and were used to determine an approximation of the surface free energy using the Owens/Wendt method.[21]

Chapter 4 : Results and Discussion

4.1 Simulant Decontamination Challenges

Decontamination experiments were run to test for simulant degradation on each of the modified coating surfaces. The coatings were prepared on pre-cleaned aluminum panels with an airbrush to ensure uniformly coated surfaces of approximately 100 µm thickness. The coatings were allowed to cure for 24 hours at ambient temperatures prior to experimentation. The coatings were modified with a final 1% w/w additive to paint ratio. The simulants were applied to the surfaces in 0.5 µL aliquots and allowed to reside on the surfaces at room temperature under darkness for 24 hours in sealed tubes. The decontamination experiments were all run in triplicate to determine the percent reduction and standard deviation of the simulants compared to a control sample. The control sample was a panel coated with unmodified MIL-PRF-85285 and exposed to the simulants for the same 24 hour period under the same conditions. The percent reductions were determined by peak area analysis of the simulant peak from the GC chromatographs of the control and modified MIL-PRF-85285 experiments. Equation 4.1 was used in calculating the percent reductions of each simulant challenge based upon the peak areas observed in the GC chromatogram.

$$Percent\ Reduction = \frac{(Peak\ Area\ of\ Control - Peak\ Area\ of\ Sample)}{Peak\ Area\ of\ Control} \times 100 \quad \text{Equation (4.1)}$$

Figure 4.1 shows the percent reduction data acquired from the simulant challenge experiments when MIL-PRF-85285 was modified with metal oxide nanoparticles (MONPs).

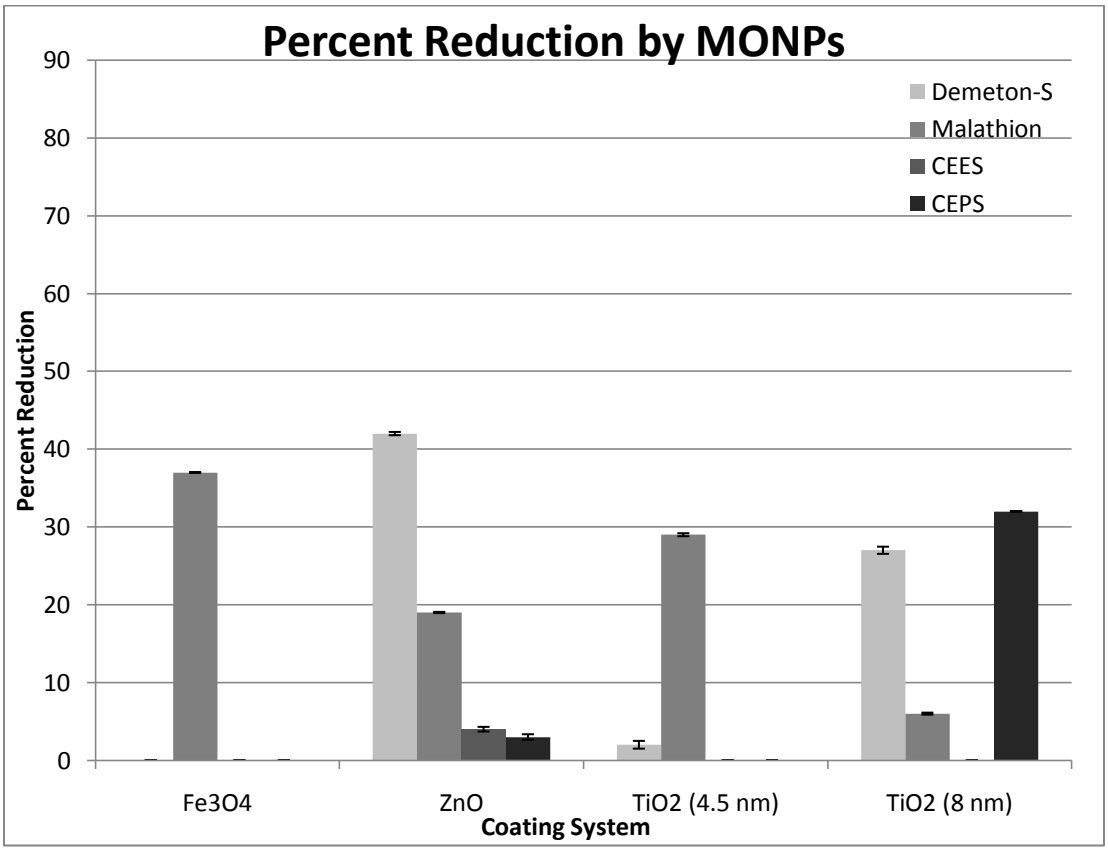

Figure 4.1: Percent reduction chart for simulant challenges against MONP modified coating systems

The results show that reduction of at least one simulant occurred on each of the modified coating systems with the zinc oxide (ZnO) modified coating showing percent reductions of all simulants to a small degree. The low percent reductions observed with

MONP modified coatings were not significant enough to promote further research as continuous self-decontamination coating additives.

Figure 4.2 shows the percent reduction data acquired from the simulant challenge experiments when MIL-PRF-85285 was modified with polyoxometallates (POMs). Table 4.1 lists the formulas of the POM additives in relation to the labels shown in Figure 4.2.

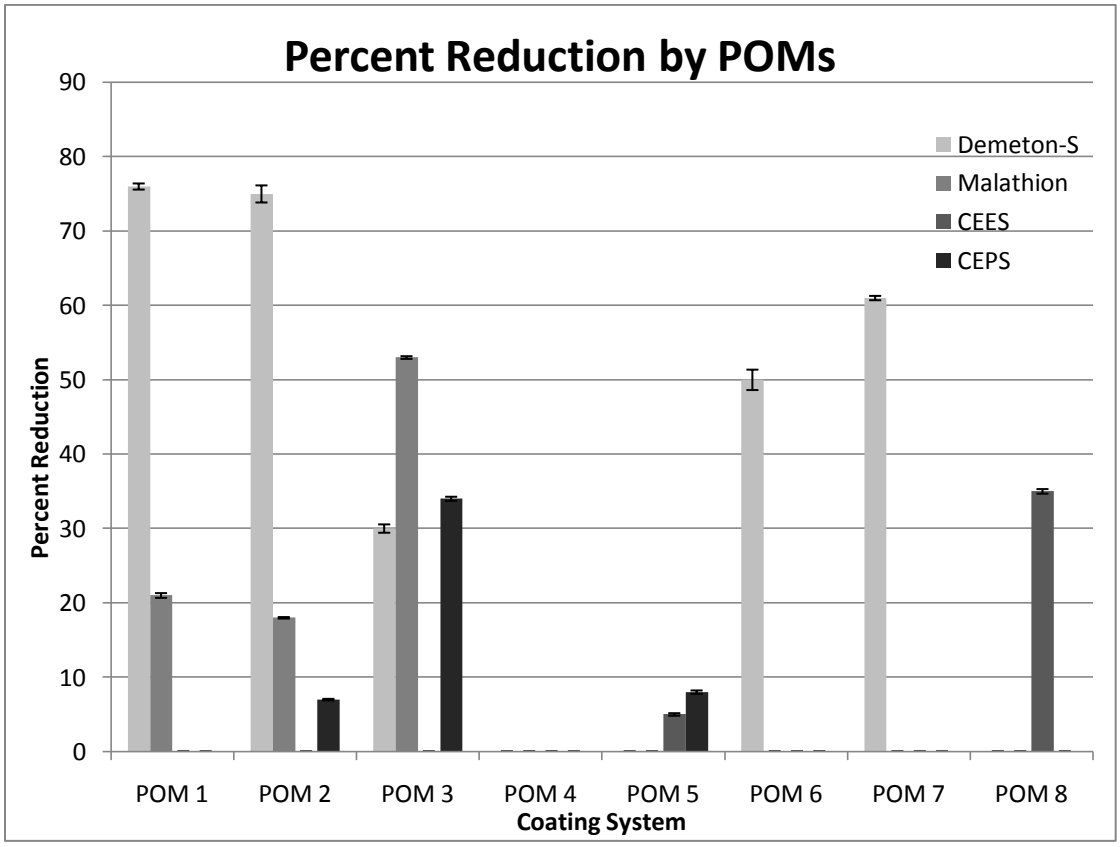

Figure 4.2: Percent reduction chart for simulant challenges against POM modified coating systems

Table 4.1: The chemical formulas of the polyoxometallates

POM #	POM Name
POM 1	α_2-$K_8P_2W_{17}O_{61}(Co^{2+}\cdot OH_2)\cdot 16H_2O$
POM 2	α_2-$K_7P_2W_{17}O_{61}(Fe^{3+}\cdot OH_2)\cdot 8H_2O$
POM 3	α-$K_8P_2W_{17}O_{61}(Ni^{2+}\cdot OH_2)\cdot 17H_2O$
POM 4	α_2-$[(n\text{-}C_4H_9)_4N]_9P_2W_{17}O_{61}(Ni^{2+}\cdot Br)$
POM 5	α/β-$K_6P_2W_{18}O_{62}\cdot 10H_2O$
POM 6	$[Fe^{II}(bpy)_3][PW_{11}O_{39}Fe_2^{III}(OH)(bpy)_2]\cdot 12H_2O$
POM 7	$(Hdmbpy)_2[Fe^{II}(dmbpy)_3]_2[(PW_{11}O_{39})_2Fe_4^{III}O_2(dmbpy)_4]\cdot 14H_2O$
POM 8	$[N(CH_3)_4]_{10}[(PW_{11}O_{39})_2Fe_2^{III}O]\cdot 12H_2O$

The results indicate that two of the POM modified coatings systems (POM 2 and POM 3) exhibited moderate to very good decontamination capabilities against three of the four simulants. The decontamination of CWA simulant CEES seemed to be non-existent for all but two of the modified coatings (POM 5 and POM 8). The two coating systems based on POM 2 and POM 3 additives could be considered as candidates for future work based upon their broader decontamination abilities as exhibited in Figure 4.2. The system modified with POM 3 would probably be the better choice because of the elevated reactivity exhibited toward the three CWA simulants with percent reductions between 30% and 53%.

Figure 4.3 shows the percent reduction data acquired from the simulant challenge experiments when MIL-PRF-85285 was modified with metal functionalized cyclodextrins.

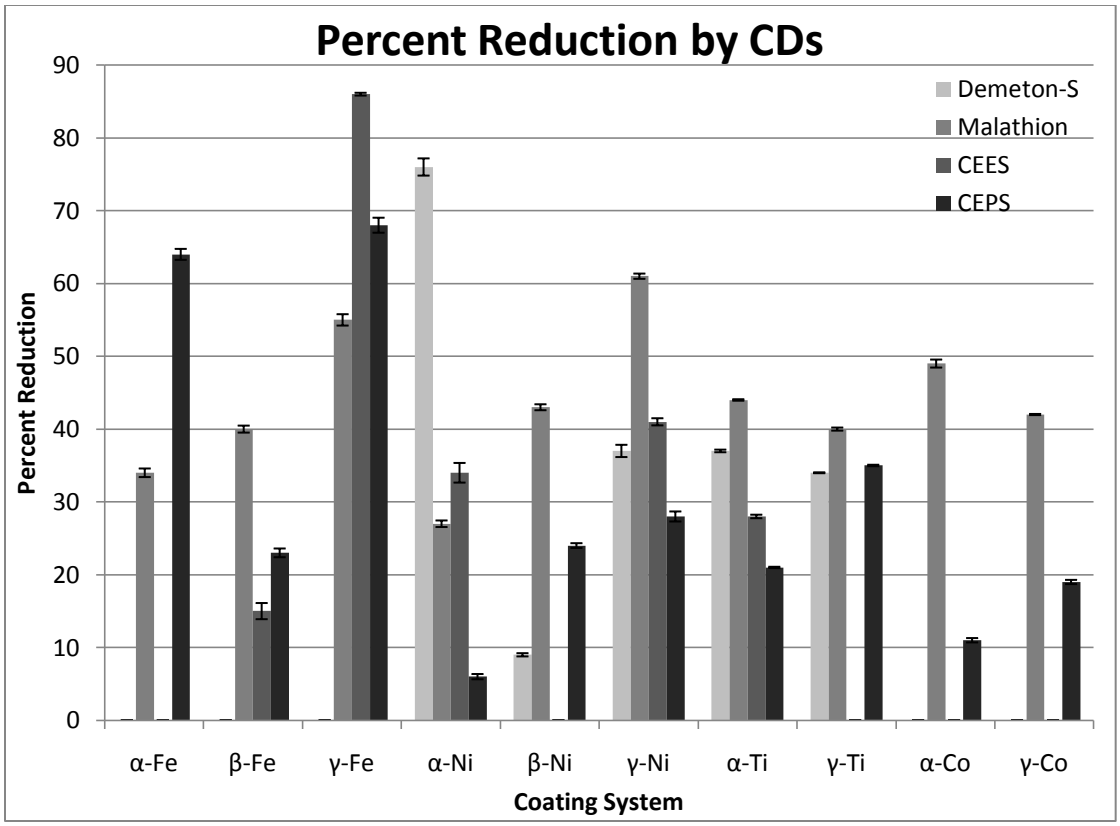

Figure 4.3: Percent reduction chart for simulant challenges against metal functionalized CD modified coating systems

The results show moderate to very good percent reductions of the CWA simulants for several of the modified coatings. Specifically the iron modified γ-CD (γ-Fe) and the nickel modified γ-CD (γ-Ni) showed the best results for decontamination overall. The coating modified with γ-Fe showed the best overall results for decontamination of CEES and CEPS with percent reductions of 86% and 68% respectively, but γ-Fe showed 0% reduction of Demeton-S which potentially reduces the utility of the compound as a coating additive. The γ-Ni modified coating showed broad range decontamination over all of the CWA simulants with percent reductions between 28% and 61% for all

simulants. This broad range decontamination capability shows that γ-Ni could be considered as a good candidate for a broad range decontamination additive.

Overall, the modified coatings exhibited decontamination capabilities when exposed to CWA simulants. The best results were exhibited by the POMs and the metal functionalized CDs coatings. The MONP modified coatings showed some decontamination capabilities however there was no individual MONP that displayed significant decontamination for multiple CWA simulants. The best selection from the POM decontamination data would be POM 3 (α-$K_8P_2W_{17}O_{61}(Ni^{2+}\cdot OH_2)\cdot 17H_2O$) based upon the broad reactivity against three of the four CWA simulants with percent reductions ranging from 30% to 53%. The modified coating which exhibited the best overall reactivity was the γ-Ni modified coating which showed decent reactivity for all of the CWA simulants. The percent reductions exhibited by γ-Ni were between 28% and 61% for all simulants. The second best coating for the metal functionalized CDs was γ-Fe which exhibited a percent reduction high of 86% for decontamination of CEES with a 68% reduction of CEPS. Due to the lack of decontamination exhibited by γ-Fe toward Demeton-S the additive γ-Ni was considered the top prospect.

4.2 Coatings Characterization

The development of a continuous self-decontamination coating against CWAs and CWA simulants requires modification to the overall coating. MIL-PRF-85285 has a specific set of standards which need to be adhered to in order to fit military

requirements. The modified coating systems were therefore tested for changes in the glass transition temperature (T_g) and surface free energy approximation.

4.2.1 Glass Transition Temperature

The T_g for all of the modified coatings was determined using differential scanning calorimetry (DSC) as discussed in Chapter 2 Section 2.5. Figure 4.4 shows the results from the DSC analysis for all of the modified coating systems.

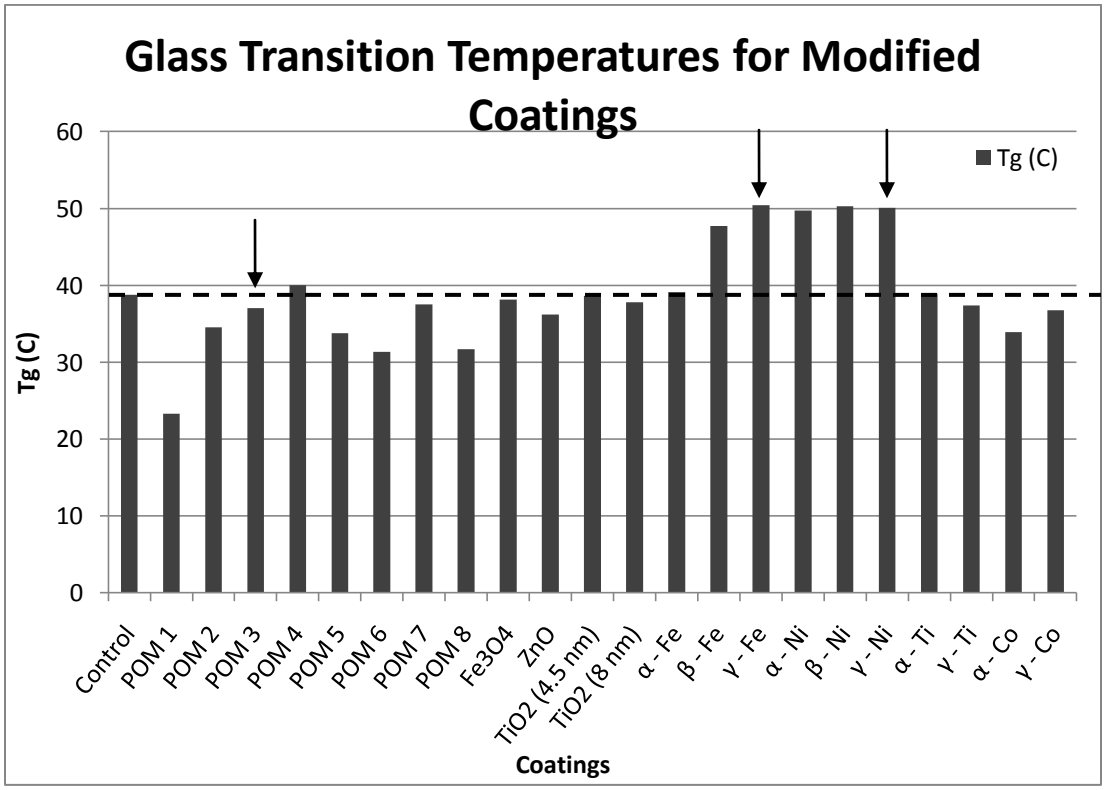

Figure 4.4: Glass transition temperature data for all of the modified coatings relative to the control coating

The data shows that both of the cyclodextrin modified coatings exhibit higher T_g values, 50.4 °C for γ-Fe and 50.1 °C for γ-Ni, than that of the control coating with a T_g value of 38.8°C. This indicates that the modified coatings are harder than the original MIL-PRF 85285 meaning the functional temperature range shifts to higher temperatures. The POM 3 modified coating had a T_g value of 37.06 °C which was slightly below that of the control T_g indicating the modified coating is slightly softer than MIL-PRF-85285.

The results from the T_g analysis indicate that the modified coatings did show signs of change upon addition of the reactive additives. The cyclodextrin additives raised the T_g value for MIL-PRF-85285 up by approximately 11 °C therefore shifting the functional temperature range up. The shift in T_g to a higher value means the modified coatings are harder than the original MIL-PRF-85285 and possibly more brittle. Based upon the location of current military action the elevation of the functional temperature range would be preferential over a coating exhibiting a shift to a lower functional temperature range. The shift exhibited in T_g by the addition of POM 3 only slightly decreased the value by approximately 1 °C making the modified coating slightly softer. The shift in T_g seems negligible and the coating should maintain a similar functional temperature range to that of the original MIL-PRF-85285.

4.2.2 Surface Free Energy Approximation

The surface free energy approximation for the modified coatings was performed using contact angle analysis as discussed in Chapter 2 Section 2.6. Figure 4.5 shows the surface free energy approximation data acquired using the Owens/Wendt method.

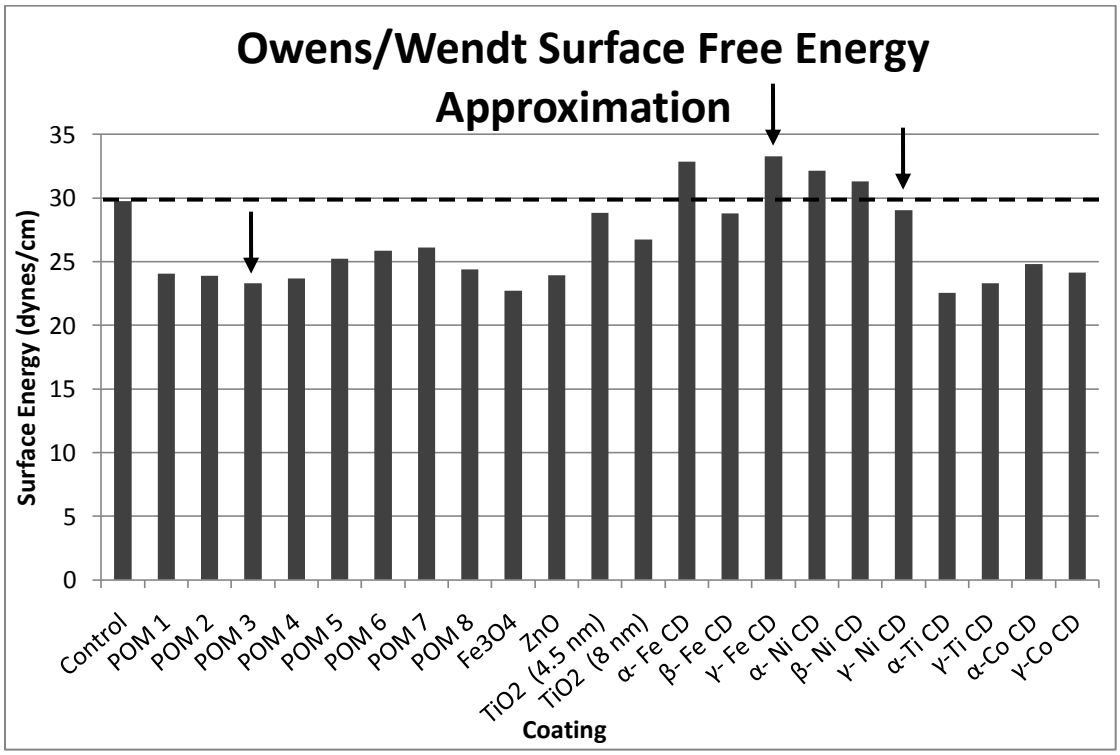

Figure 4.5: Owens/Wendt surface free energy approximations for all of the modified coatings relative to the control coating

The data shows that the surface free energy approximations for the two cyclodextrin modified coatings of interest are slightly different from the control (29.77 dynes/cm). The γ-Fe CD modified coating had an elevated surface free energy approximation of 33.27 dynes/cm relative to the control. This indicates that the surface

will interact better with the solvents of higher surface tension and allow more wetting than the control. The γ-Ni CD modified coating had a slightly lowered surface free energy approximation of 29.05 dynes/cm relative to the control coating and therefore the solvents will bead up more on the modified surface than that of the MIL-PRF-85285. The POM 3 coating exhibited a larger decrease in the surface free energy approximation to 23.29 dynes/cm which is approximately a 6 dyne/cm difference from the MIL-PRF-85285. The change exhibited by the POM 3 modified coating indicates that more solvents will bead up on the surface and have less contact area with the reactive surface.

The surface free energy approximation data provides information of how solvents, CWA simulants and CWAs will interact with the surface. The γ-Fe CD exhibited an increase in the surface free energy approximation relative to MIL-PRF-85285 indicating that the modified coating will allow the solvent to spread more when in contact with the surface. More surface-liquid contact area means more contact with the reactive additives and more opportunities for decontamination. The γ-Ni CD modified coating produced a reduction in the surface free energy approximation from MIL-PRF-85285 which would cause the solvents in contact with the surface to bead up reducing surface-liquid contact area. The decrease in surface-liquid contact area means a reduction in the contact time with the reactive additives and could slow decontamination processes. The last coating of interest is the POM 3 modified coating which exhibited a larger decrease in the surface free energy approximation. The larger

decrease indicates that the surface will have even less contact area with solvent residing on the surface and fewer interactions will occur with the additives increasing the decontamination time even more.

Chapter 5 : Conclusions

The current research has developed a series of reactive additives for utilization in coatings in an effort to create a continuous self-decontamination surface. The research has shown that coatings modified with low percentages of additives (1% w/w) POMs and metal functionalized CDs can decontaminate CWA simulants CEES, CEPS, Malathion, and Demeton-S with a high degree of success. The use of MONPs was also tested because of their characteristically cheap and easy productions however little decontamination success was achieved using these additives.

The underlying goal of the research was the development of cheap and easy to synthesize reactive additives. These additives needed to be effective decontamination agents when incorporated into a coating without changing the physical properties exhibited by the base coatings. The two additives classes showing the greatest success against CWA simulant challenges offer moderate synthetic pathways for production. The synthesis of POM 3 involved standard bench top chemistry practices without the need for specialized glassware or materials. The major drawback to the synthesis of POM 3 was the multi-step isolation of the pure alpha-2 isomer before incorporation of the hetero-metal which resulted in lower overall percent yields of the final product. The synthesis of the metal functionalized cyclodextrins offered a more stringent synthetic pathway compared to POM 3 however fewer steps were required, greatly increasing the percent yields compared to the POM 3 synthesis.

Future work focusing on different modifications to POMs and CDs would be the direction to pursue since the greatest success was achieved with these additives. Broadening the range of transition metals as well as incorporation of different organic substituent groups could help increase the reactivity toward simulants and CWAs. Modification of coatings with multiple additives could also prove to be useful as well since no single additive was highly successful against all of the simulant challenges.

References

(1) Tu, A. T. *J. Mass Spectrom. Soc. Jpn.* **1996**, *44*, 293.

(2) Yang, Y.-C. *Acc. Chem. Res.* **1999**, *32*, 109.

(3) Talmage, S. S.; Watson, A. P.; Hauschild, V.; Munro, N. B.; King, J. *Curr. Org. Chem.* **2007**, *11*, 285.

(4) Yang, Y. C.; Baker, J. A.; Ward, J. R. *Chem. Rev.* **1992**, *92*, 1729.

(5) Yebra, D. M.; Kiil, S.; Dam-Johansen, K. *Progress in Organic Coatings* **2004**, *50*, 75.

(6) Fulmer, P. A.; Lundin, J. G.; Wynne, J. H. *ACS Appl. Mater. Interfaces* **2010**, *2*, 1266.

(7) Szinicz, L. *Toxicology* **2005**, *214*, 167.

(8) Slotten, H. R. *The Journal of American History* **1990**, *77*, 476.

(9) Random, H. *Random House Webster's college dictionary*; Random House: New York, 2001.

(10) Sayer, N. M.; Whiting, R.; Green, A. C.; Anderson, K.; Jenner, J.; Lindsay, C. D. *J. Chromatogr., B: Anal. Technol. Biomed. Life Sci.* **2010**, *878*, 1426.

(11) Cook, J. R.; Van, B. R. G. *Toxicol. Pathol.* **1997**, *25*, 481.

(12) Amitai, G.; Adani, R.; Hershkovitz, M.; Bel, P.; Rabinovitz, I.; Meshulam, H. *J. Appl. Toxicol.* **2003**, *23*, 225.

(13) Liu, J.; Powell, K. L.; Thames, H. D.; MacLeod, M. C. *Chem. Res. Toxicol.* **2010**, *23*, 488.

(14) Atkins, K. B.; Lodhi, I. J.; Hurley, L. L.; Hinshaw, D. B. *J. Appl. Toxicol.* **2000**, *20*, S125.

(15) Marrs, T. C. *Pharmacol. Ther.* **1993**, *58*, 51.

(16) Aurbek, N.; Thiermann, H.; Szinicz, L.; Eyer, P.; Worek, F. *Toxicology* **2006**, *224*, 91.

(17) Barakat, N. H.; Zheng, X.; Gilley, C. B.; MacDonald, M.; Okolotowicz, K.; Cashman, J. R.; Vyas, S.; Beck, J. M.; Hadad, C. M.; Zhang, J. *Chem. Res. Toxicol.* **2009**, *22*, 1669.

(18) Bizzigotti, G. O.; Castelly, H.; Hafez, A. M.; Smith, W. H. B.; Whitmire, M. T. *Chemical Reviews* **2008**, *109*, 236.

(19) Salter, B.; Owens, J.; Hayn, R.; McDonald, R.; Shannon, E. *J. Mater. Sci.* **2009**, *44*, 2069.

(20) Smith, B. M. *Chem. Soc. Rev.* **2008**, *37*, 470.

(21) Owens, D. K.; Wendt, R. C. *J. Appl. Polym. Sci.* **1969**, *13*, 1741.

(22) Zisman W, A. Relation of the Equilibrium Contact Angle to Liquid and Solid Constitution. In *Contact Angle, Wettability, and Adhesion*; AMERICAN CHEMICAL SOCIETY, 1964; Vol. 43; pp 1.

(23) Bartelt-Hunt, S. L.; Knappe, D. R. U.; Barlaz, M. A. *Crit. Rev. Environ. Sci. Technol.* **2008**, *38*, 112.

(24) Mizrahi, D. M.; Saphier, S.; Columbus, I. *J. Hazard. Mater.* **2010**, *179*, 495.

(25) Okun, N. M.; Tarr, J. C.; Hilleshiem, D. A.; Zhang, L.; Hardcastle, K. I.; Hill, C. L. *J. Mol. Catal. A: Chem.* **2006**, *246*, 11.

(26) Okun, N. M.; Anderson, T. M.; Hill, C. L. *J. Mol. Catal. A: Chem.* **2003**, *197*, 283.

(27) Yang, Y.-C.; J. Berg, F.; L. Szafraniec, L.; T. Beaudry, W.; A. Bunton, C.; Kumar, A. *Journal of the Chemical Society, Perkin Transactions 2* **1997**, 607.

(28) Wagner, G. W.; Sorrick, D. C.; Procell, L. R.; Brickhouse, M. D.; McVey, I. F.; Schwartz, L. I. *Langmuir* **2007**, *23*, 1178.

(29) Wagner, G. W.; Yang, Y.-C. *Ind. Eng. Chem. Res.* **2002**, *41*, 1925.

(30) Abbott, A.; Sierakowski, T.; Kiddle, J. J.; Clark, K. K.; Mezyk, S. P. *J. Phys. Chem. B* **2010**, *114*, 7681.

(31) Bromberg, L.; Schreuder-Gibson, H.; Creasy, W. R.; McGarvey, D. J.; Fry, R. A.; Hatton, T. A. *Ind. Eng. Chem. Res.* **2009**, *48*, 1650.

(32) Niederberger, M.; Garnweitner, G. *Chem.--Eur. J.* **2006**, *12*, 7282.

(33) Niederberger, M. *Accounts of Chemical Research* **2007**, *40*, 793.

(34) Wagner, G. W.; Bartram, P. W.; Koper, O.; Klabunde, K. J. *J. Phys. Chem. B* **1999**, *103*, 3225.

(35) Wagner, G. W.; Koper, O. B.; Lucas, E.; Decker, S.; Klabunde, K. J. *J. Phys. Chem. B* **2000**, *104*, 5118.

(36) Wagner, G. W.; Chen, Q.; Wu, Y. *J. Phys. Chem. C* **2008**, *112*, 11901.

(37) Hatton, T. A.; Bromberg, L. E. Catalytic nanoparticles for nerve agent destruction; Massachusetts Institute of Technology, USA . 2007; pp 128 pp.

(38) Hatton, T. A.; Bromberg, L. E. Catalytic nanoparticles for nerve agent destruction; Massachusetts Institute of Technology, USA . 2009; pp 36pp.

(39) Bilecka, I.; Djerdj, I.; Niederberger, M. *Chem. Commun. (Cambridge, U. K.)* **2008**, 886.

(40) Niederberger, M.; Bartl, M. H.; Stucky, G. D. *Chem. Mater.* **2002**, *14*, 4364.

(41) Katsoulis, D. E. *Chem. Rev. (Washington, D. C.)* **1998**, *98*, 359.

(42) Guo, Y.; Wang, Y.; Hu, C.; Wang, Y.; Wang, E.; Zhou, Y.; Feng, S. *Chem. Mater.* **2000**, *12*, 3501.

(43) Vazylyev, M.; Sloboda-Rozner, D.; Haimov, A.; Maayan, G.; Neumann, R. *Top. Catal.* **2005**, *34*, 93.

(44) Hiskia, A.; Troupis, A.; Antonaraki, S.; Gkika, E.; Papaconstantinou, P. K. *Int. J. Environ. Anal. Chem.* **2006**, *86*, 233.

(45) Lyon, D. K.; Miller, W. K.; Novet, T.; Domaille, P. J.; Evitt, E.; Johnson, D. C.; Finke, R. G. *J. Am. Chem. Soc.* **1991**, *113*, 7209.

(46) Pichon, C.; Dolbecq, A.; Mialane, P.; Marrot, J.; Riviere, E.; Goral, M.; Zynek, M.; McCormac, T.; Borshch, S. A.; Zueva, E.; Secheresse, F. *Chem.--Eur. J.* **2008**, *14*, 3189.

(47) Johnson, R. P.; Hill, C. L. *J. Appl. Toxicol.* **1999**, *19*, S71.

(48) Auletta, T.; De, J. M. R.; Mulder, A.; Van, V. F. C. J. M.; Huskens, J.; Reinhoudt, D. N.; Zou, S.; Zapotoczny, S.; Schoenherr, H.; Vancso, G. J.; Kuipers, L. *J. Am. Chem. Soc.* **2004**, *126*, 1577.

(49) Dyck, A. S. M.; Kisiel, U.; Bohne, C. *J. Phys. Chem. B* **2003**, *107*, 11652.

(50) Velic, D.; Knapp, M.; Kohler, G. *J. Mol. Struct.* **2001**, *598*, 49.

(51) Szejtli, J. *Chemical Reviews* **1998**, *98*, 1743.

(52) Takeo, K.; Uemura, K.; Mitoh, H. *J. Carbohydr. Chem.* **1988**, *7*, 293.

(53) Takeo, K.; Mitoh, H.; Uemura, K. *Carbohydr. Res.* **1989**, *187*, 203.

(54) Fugedi, P. *Carbohydr. Res.* **1989**, *192*, 366.

(55) Kirschner, D.; Jaramillo, M.; Green, T.; Hapiot, F.; Leclercq, L.; Bricout, H.; Monflier, E. *J. Mol. Catal. A: Chem.* **2008**, *286*, 11.

(56) Barr, L.; Easton, C. J.; Lee, K.; Lincoln, S. F.; Simpson, J. S. *Tetrahedron Lett.* **2002**, *43*, 7797.

(57) Bellia, F.; La, M. D.; Pedone, C.; Rizzarelli, E.; Saviano, M.; Vecchio, G. *Chem. Soc. Rev.* **2009**, *38*, 2756.

(58) Cabal, J.; Kuca, K.; Sevelova-Bartosova, L.; Dohnal, V. *Acta Med. (Hradec Kralove, Czech Rep.)* **2004**, *47*, 115.

(59) Contant, R. *Can. J. Chem.* **1987**, *65*, 568.

(60) Bandwar, R. P.; Rao, C. P. *Carbohydr. Res.* **1997**, *297*, 341.

(61) Bandwar, R. P.; Sastry, M. D.; Kadam, R. M.; Rao, C. P. *Carbohydr. Res.* **1997**, *297*, 333.

(62) Kaiwar, S. P.; Rao, C. P. *Carbohydr. Res.* **1992**, *237*, 203.

(63) Wunderlich, B. *J. Appl. Polym. Sci.* **2007**, *105*, 49.